# EXPERIMENT 06

# Helium Neon Laser

**Panel 1 (energy level diagram):**

Helium | Neon

Energy eV

21

$2\,^1S_0$

Collision He->Ne

3s

20

$2\,^3S_1$

Laser transition

632 nm

19

Electron Impact

2p

18

spontaneous Emission

17

1s

recombination impact

0

$1\,^1S_0$

**Panel 3 (apparatus diagram):**

F  A  B  C  D  E

H  G

TUBE CURRENT  2.8

LASER POWER  1.37

LASER  P  TC-01

**Panel 5 (prism diagram):**

Prism

Littrow Prism

Mirror Coating

$\beta$  $\alpha$  $\gamma$  $\omega$

$\beta$  $\alpha$  $\gamma$  $\omega$

Arrangement within the Laser Resonator

**Panel 6:**

MEOS

# 1 Introduction

The Helium-Neon laser was the first continuous laser. It was invented by Javan et. al. in 1961. Nowadays lasers are usually pre-adjusted using a He-Ne laser. But how did Javan manage to do this? This shows that it is no coincidence that Javan's first He-Ne laser oscillated at a wavelength of 1.5μm, since the amplification at this wavelength is considerably higher than the 632 nm line which is reached at what is now commonly known as the red line, which was made to oscillate only one year later by White and Ridgen. The similarity between the manufacturing techniques of He-Ne lasers and electron valves helped in the mass production and distribution of He-Ne lasers. The replacement of tubes by transistors in the sixties left a sufficiently redundant production capacity. In Germany for example, the Siemens tube factory took over this production and has produced over one million He-Ne lasers to date.

It is now clear that He-Ne lasers will have to increasingly compete with laser diodes in the future. But He-Ne lasers are still unequalled as far as beam geometry and the purity of the modes are concerned. Laser diodes will have to be improved to a great extent before they pose a serious threat to He-Ne lasers.

# 2 Fundamentals

## 2.1 He-Ne energy- level diagram

The fascination for inert gases and their clear atomistic structure formed the basis for many spectroscopic investigations. The knowledge obtained through spectroscopic data was extremely helpful in deciding to choose helium and neon for the first lasers, using Schawlow Towne's discovery of lasing conditions in 1958 to estimate whether an inversion was feasible in laser operation. The lifetime of the s- and p-states were well known. Those of the s-states were longer than those of the p-states by a factor of about 10. The inversion condition was therefore fulfilled.
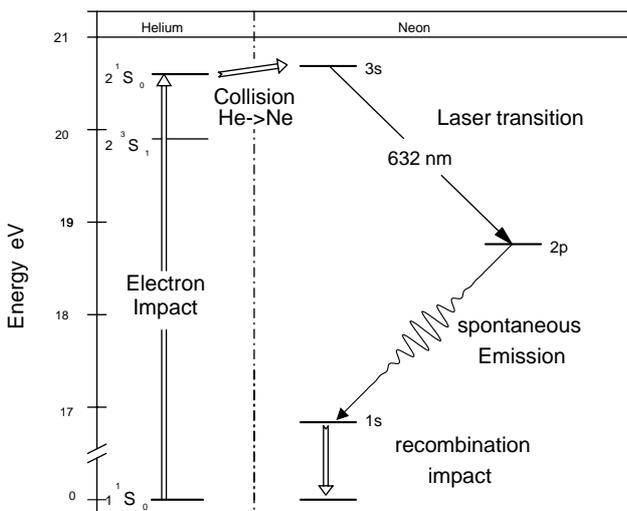


**Fig. 1: Excitation and Laser process for the visible Laser emission**

Fig. 1 shows the reduced energy-level diagram for helium and neon. Only those levels important in the discussion of

the excitation and laser processes at a wavelength of 632 nm are indicated.

The left side of the representation shows the lower levels of the helium atoms. Observe how the energy scale is interrupted and that there is a larger difference in energy in the recombination process than is evident in the diagram. Paschen's names for the neon energy levels are used (Racah's term descriptions are often found as well). The terms are simply numbered consecutively, from bottom to top. A characteristic of helium is that its first states to be excited, $2^1S_1$ and $2^1S_0$ are metastable, i.e. optical transitions to the ground state $1^1S_0$ are not allowed, because this would violate the selection rules for optical transitions. As a result of gas discharge, these states are populated by electron collisions (collision of the second type, Fig. 2).

A collision is called a collision of the second type if one of the colliding bodies transfers energy to the other so that a transition from the previous energy state to the next higher or lower takes place. Apart from the electron collision of the second type there is also the atomic collision of the second type. In the latter, an excited helium atom reaches the initial state because its energy has been used in the excitation of a Ne atom. Both these processes form the basis for the production of a population inversion in the Ne system.
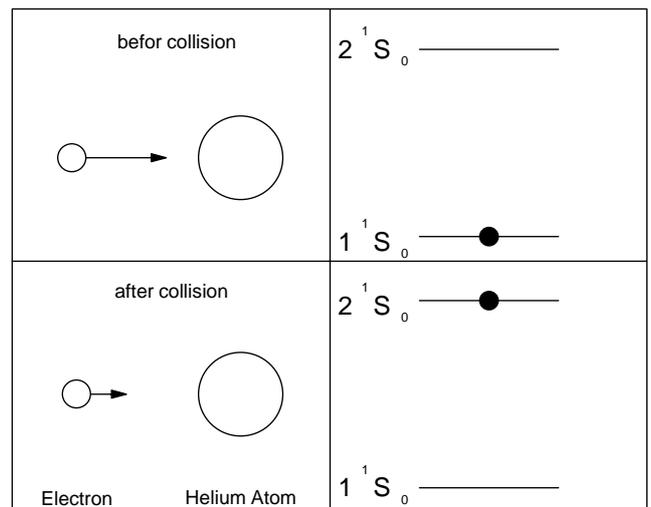


**Fig. 2: Electron collision of the second kind**

If we look at Fig. 1 we can see that the $2^1S_0$ is slightly below the 3s level of the neon. However, the additional thermal energy kT is sufficient to overcome this gap.

As already mentioned, the lifetime of the s-states of the neon are approximately 10 times longer as those of the p-states. An immediate population inversion between the 3s and the 2p levels will therefore be generated. The 2s level is emptied due to spontaneous emission into the 1s level. After this the neon atoms reaching their ground state again, primarily through collisions with the tube wall (capillary), since an optical transition is not allowed. This calming down process is the bottle neck in the laser cycle. It is therefore advisable to choose a capillary diameter that is as small as possible. However, the laser will then suffer more losses. Modern He-Ne lasers work at an optimum of these contradictory conditions. This is the main reason for the comparatively low output of He-Ne lasers.

We have discussed the laser cycle of the commonly known red line at 632 nm up to this point. However the neon has several other transitions, used to produce about 200 laser lines in the laboratories. The following explanation describes the energy-level diagram for further visible lines. After that infrared laser transitions will be discussed.
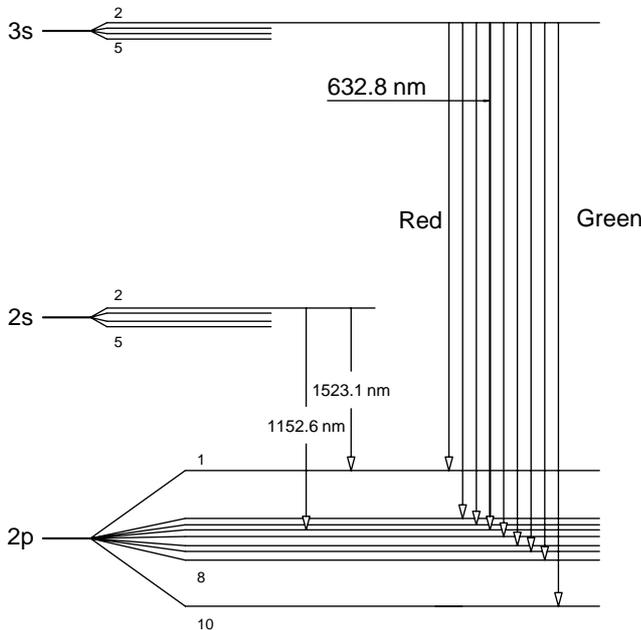


**Fig. 3: The most important laser transitions in the neon system**

The 3s state is populated by Helium atoms of the $2^1S_0$, state as a result of an atomic collision. The 3s state consists of 4 sub-states out of which it is primarily the $3s_2$ state which has been populated through the collision process. The population density of the other 3s sub-states is app. 400 times less than that of the $3s_2$ state. The 2s state is populated by the Helium atoms of the $2^3S_1$, as a result of an atomic collision.

The four sub-states of the 2s group are all populated in a similar way. Visible (VIS) optical transitions and laser processes are taking place between the 3s2→2pi and infrared (IR) between the 2si→2pi energy levels.

The following table shows the most important laser transitions. The Einstein coefficients $A_{ik}$ are given for the visible lines and amplification is indicated as a percentage per meter.

Further laser transitions are known, which start at the 3s2 level and terminating at the 3p level of the neon. However, these laser transitions lie even further within the infrared spectral range and cannot be detected with the silicon detector used in the experiment. They are not particularly suitable for experiments. Notice that these lines are originating from the same level as the visible lines and are therefore competing with them. Since the cross-section of the stimulated emission is increasing with $\lambda^3$ as well, the amplification of these lines is therefore very strong. This applies to the 3.39 μm line in particular, which, due to a sufficiently long capillary, shows laser activity (so called super fluorescence) even without an optical resonator.

| Transition | Wavelength [nm] | $A_{ik}$ [$10^8$ s$^{-1}$] | Gain [%/m] |
|---|---|---|---|
| 3s2→2p1 | 730.5 ③ | 0,00255 | 1,2 |
| 3s2→2p2 | 640.1 ① | 0,0139 | 4,3 |
| 3s2→2p3 | 635.2 ① | 0,00345 | 1,0 |
| 3s2→2p4 | 632.8 ① | 0,0339 | 10,0 |
| 3s2→2p5 | 629.4 ① | 0,00639 | 1,9 |
| 3s2→2p6 | 611.8 ① | 0,00226 | 1,7 |
| 3s2→2p7 | 604.6 | 0,00200 | 0,6 |
| 3s2→2p8 | 593.9 | 0,00255 | 0,5 |
| 3s2→2p9 | ★ | | |
| 3s2→2p10 | 543.3 | 0,00283 | 0,52 |
| 2s2→2p1 | 1523.1 ② | | |
| 2s2→2p2 | 1177.0 ③ | | |
| 2s2→2p3 | 1160.5 | | |
| 2s2→2p4 | 1152.6 ③ | | |
| 2s2→2p5 | 1141.2 ③ | | |
| 2s2→2p6 | 1084.7 ③ | | |
| 2s2→2p7 | 1062.3 | | |
| 2s2→2p8 | 1029.8 | | |
| 2s2→2p9 | ★ | | |
| 2s2→2p10 | 886.5 | | |
| 2s3→2p2 | 1198.8 ③ | | |
| 2s3→2p5 | 1161.7 ③ | | |
| 2s3→2p7 | 1080.1 ③ | | |

**Table 1: Transitions and Laser lines**

①  Laser transitions are demonstrated in the experiment if laser tube is supplied with perpendicular or Brewster windows

②  Laser transition is demonstrated if laser tube is supplied with Brewster windows and special set of mirrors

③  Laser transitions are demonstrated in the experiment if laser tube is supplied with Brewster windows and IR mirror set

★  Transition not allowed

Appropriate measures must be taken to suppress the super fluorescence to avoid a negative influence on the visible laser lines.
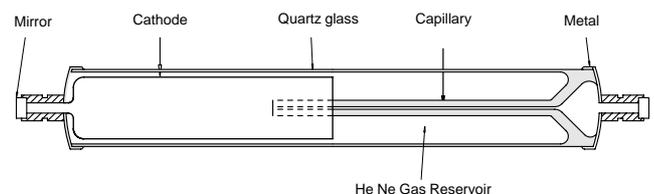


**Fig. 4: Modern He-Ne laser with glass-to-metal soldering of the anode, cathode and laser mirror**

Fig. 4 shows a modern laser tube made with highly perfected manufacturing techniques and optimised to suit the physical aspects of the laser. This applies to the resonator in particular, which is designed for a best possible

output in the fundamental mode with a purely Gaussian beam and spectral purity in single mode operation (e.g. for interferometric length measurement). The fulfilment of this demand depends, amongst other aspects, on the optimal adaptation of the resonator to the amplification profile of the Neon. The behaviour of Neon during amplification will therefore be discussed first.

### *2.2 Amplification of the Neon atoms*

The Neon atoms move more or less freely in the laser tube but at different speeds. The number N of neon atoms with the mass m, within a speed interval of v to v+dv is described according to the Maxwell-Boltzmann distribution (Fig. 5).

$$\frac{n(v)}{N} = \frac{4}{\sqrt{\pi}} \cdot \frac{v^2}{\sqrt[3]{(2kT/m)^2}} \cdot e^{-\frac{mv^2}{k \cdot T}} dv$$

T is the absolute temperature and k Boltzman´s constant The above equation is applicable for all directions in space. However, we are only interested in the distribution of speed in the direction of the capillary. Using $v^2 = v_x^2 + v_y^2 + v_z^2$ we obtain for the direction x:

$$\frac{n(v_x)}{N} = \sqrt{2kT/m} \cdot e^{-\frac{m \cdot v^2}{k \cdot T}} dv_x \qquad \textbf{Eq. 2.1}$$

A resting observer will now see the absorption or emission frequency shifted, due to Doppler's effect (Ch.Doppler: Abh. d. K. Boehmischen Ges.d.Wiss. (5). Vol.II (1842) P.465), and the value of the shift will be:

$$v = \frac{v_0}{1 \pm v/c} \text{ assuming } v << c \qquad \textbf{Eq. 2.2}$$

$v_0$ is the absorption or emission frequency of the resting neon atom and c the speed of light. If the Doppler equation (Eq. 2.1)is used to substitute the velocity v in the Maxwell-Boltzmann´s velocity distribution (Eq. 2.2) the line broadening produced by the movement of Neon atoms can be found. Since the intensity is proportional to the number of absorbing or emitting Neon atoms, the intensity distribution will be:

$$I(v) = I(v_0) \cdot e^{-\left(c \cdot \frac{v-v_0}{v_0 \cdot v_w}\right)^2} \qquad \textbf{Eq. 2.3}$$

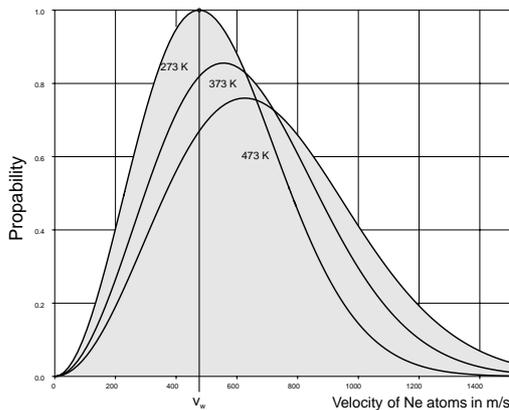$v_w$ is the most likely speed according to: $v_w = \sqrt{\dfrac{2kT}{m}}$



### Fig. 5: Probability Distribution for the velocity v of the neon atoms at an interval v to v + dv.

The full width at half maximum is calculated by setting I(v)=1/2 I($v_0$) and the result is:

$$\Delta v_{Doppler} = \sqrt{4 \cdot \ln 2} \cdot \frac{v_w}{c} \cdot v_0 \qquad \textbf{Eq. 2.4}$$

We can conclude from Eq. 2.4 that the line broadening caused by Doppler's effect is larger in the case of:

        higher resonance frequencies $v_0$
        or smaller wavelengths ($v_0=c/\lambda_0$, UV-lines)
        higher most likely velocity $v_w$
        that means higher temperature T
and smaller in the case of:

        a larger particle mass.

The line profile also corresponds to a Gaussian distribution curve (Eq. 2.3). Fig. 6 shows this kind of profile. The histogram only approaches the distribution curve when the speed intervals dv are small.
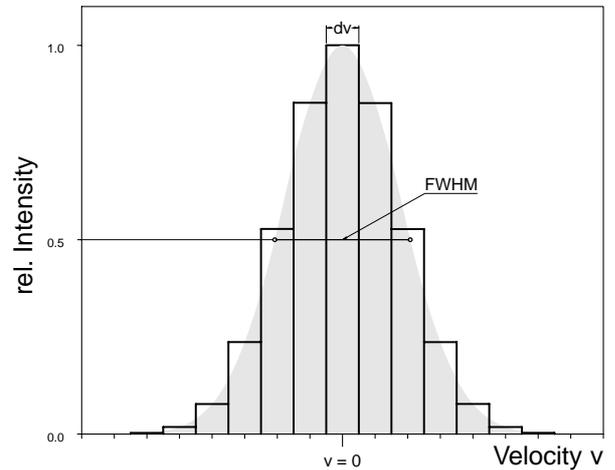


### Fig. 6: Inhomogeneous line profile, speed intervals dv

Why these speed intervals dv or frequency intervals dv you may ask. Actually there are formal reasons for this. Not having any intervals at all would be like wanting to make a statement on fishing out a particle with an exact speed or frequency from the ensemble. It is almost impossible to do. So, we define finite probabilities of ensembles by using intervals. If we succeed in this, we can make the intervals smaller and work with "smooth curves". On closer observation we can see that a line broadened by the Doppler effect actually does not have a pure Gaussian distribution curve. To understand this, we pick out an ensemble of Ne atoms whose speed components have the value v in the direction we are looking at. We expect that all these atoms emit light with the same frequency v or wavelength λ. But we have to consider an additional effect which is responsible for the natural linewidth of a transition. We know that each energy level poses a so called life time. The population $n_2$ of a state 2 decays into a state 1 with lower energy with a time constant $\tau_s$ following the equation :

$$n_2(t) = n_2(t=0) \cdot e^{-A_{21} \cdot t} \qquad \text{with } \tau_s = 1/A_{21}$$

$A_{21}$ is the famous Einstein coefficient for the spontaneous emission. The emission which takes place is termed as spontaneous emission.
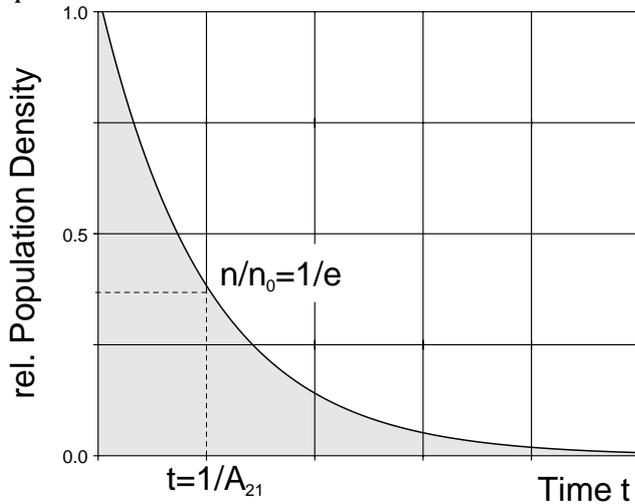


**Fig. 7: Decay of the population of state 2 into a state 1 with lower energy**

This shows us, that the ensemble of Ne atoms does not emit light at a single frequency. It emits a frequency spectra represented by an Lorentz profile (Fig. 8).

$$\delta(v) = \frac{1}{4\pi \cdot (v - v_{21})^2 + (1/2 \cdot \tau_s)^2} \ , \ v_0 \equiv v_{21}$$

The exact profile formation can be determined from the convolution of the Gaussian profile with the individual Lorentz profiles. The result obtained in this manner is called as the Voigt profile. Since one group of particles in an ensemble can be assigned to a given speed v, these groups have characteristics that differentiate them. Every group has its own frequency of resonance. Which group a photon interacts with depends on the energy (frequency) of the photon. This does not affect the other groups which are not resonant on this interaction. Therefore such kind of a gain profile is termed inhomogeneous.
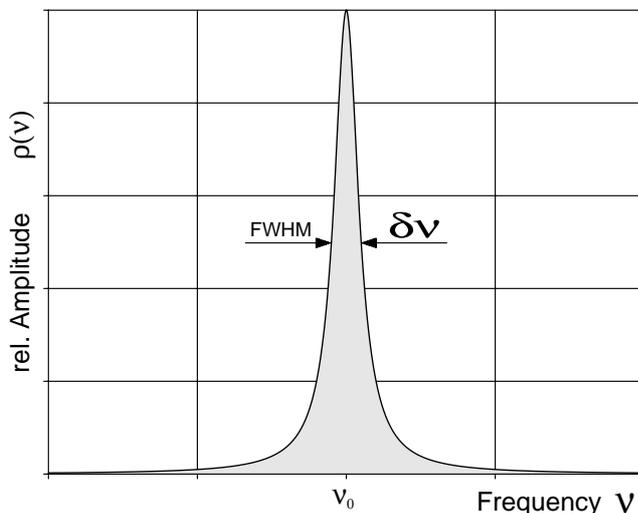


**Fig. 8: Natural linewidth (FWHM) caused by sponta-neous emission**
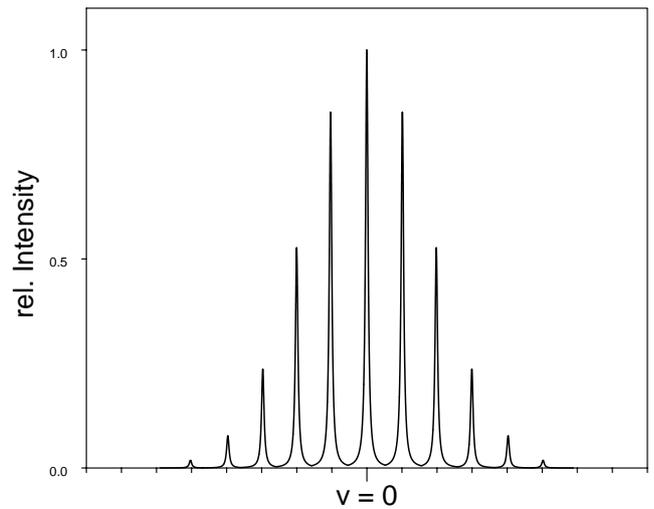


**Fig. 9: Natural broadened line profiles (homogeneous) for groups of speed v within the inhomogeneous Doppler broadened gain profile**

As we already know gain occurs in a medium when it shows inversion. This means that the population density of the upper level $n_2$ (3s in the Ne-system) is larger than the population density of the lower state $n_1$ (2p). In Fig. 10 the population profiles are rotated by 90° to draw them in the well known energy level diagram. Transition can only take place between sub-ensembles which have the same velocity v because the optical transition does not change the speed of the particular Ne atom.
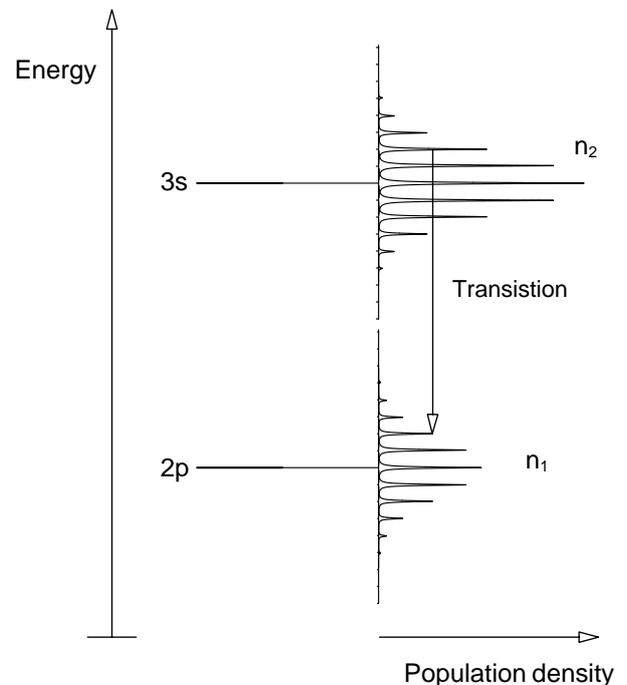


**Fig. 10: Population inversion and transition between sub-ensembles with same velocity v**

The situation of Fig. 10 shows a population inversion $n_2 >$ $n_1$. Besides some specific other constants the gain is

proportional to the difference $n_2 - n_1$. Now we will place the inverted ensemble of Ne atoms into an optical cavity, which is formed by two mirrors having the distance of L. Due to the spontaneous emission photons are generated which will be amplified by the inverted medium and reflected back from the mirrors undergoing a large number of passes through the amplifying medium. If the gain compensates for the losses, a standing laser wave will be built up inside the optical resonator. Such a standing wave is also termed as oscillating mode of the resonator also eigenmode or simply mode. Every mode must fulfil the following condition:

$$L = n \cdot \frac{\lambda}{2} \text{ or } L = n \cdot \frac{c}{2v}$$

L represents the length of the resonator, $\lambda$ the wavelength, c the speed of light, $v$ the frequency of the generated light and n is an integer number. Thus every mode has its frequency of
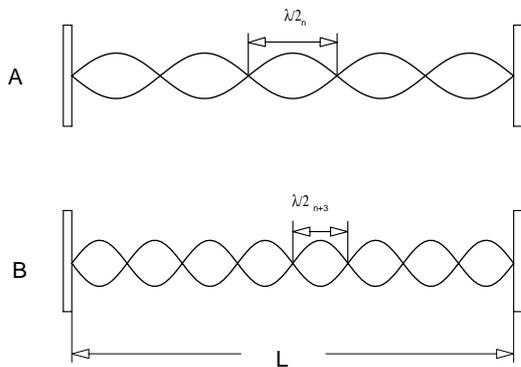
$$v(n) = n \cdot \frac{c}{2L}$$



**Fig. 11: Standing longitudinal waves in an optical reso-nator. A with n nodes and B with n+3 nodes**

e.g. A He-Ne-Laser with a resonator length of 30 cm at an emission wavelength $\lambda$ of 632.8 nm will have the following value for n:

$$n = \frac{v}{c} \cdot 2 \cdot L = 2 \cdot \frac{L}{\lambda} = 2 \cdot \frac{0,3}{632,8 \cdot 10^{-8}} = 949.167$$

The difference in frequency of two neighboured modes is:

$$\Delta v = v(n+1) - v(n) = (n+1) \cdot \frac{c}{2L} - n \cdot \frac{c}{2L} = \frac{c}{2L}$$

In the above example the distance between modes would be

$$\Delta v = \frac{3 \cdot 10^8}{2 \cdot 0,3} = 5 \cdot 10^8 \text{ Hz=500 MHz}$$

If the active laser material is now brought into the resonator standing waves will be formed due to the continuous emission of the active material in the resonator and energy will be extracted from the material. However, the resonator can only extract energy for which it is resonant. Strictly speaking, a resonator has an indefinite amount of modes, whereas the active material only emits in an area of frequency determined by the emission line width. Fig. 12 shows the situation in the case of material that is inhomogeneously broadened.
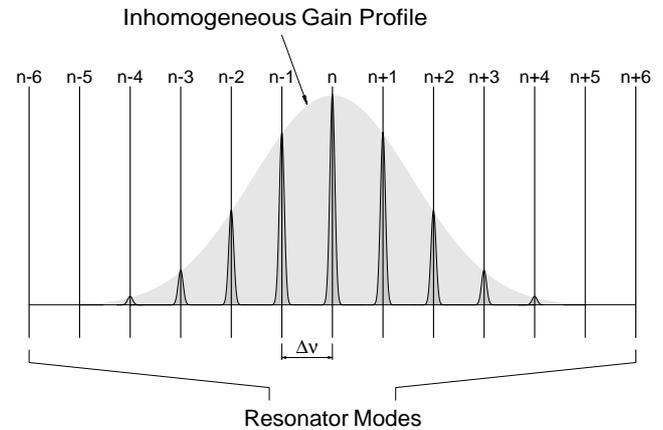


**Fig. 12: Inhomogeneous gain profile (Gaussian profile) interacting with an optical resonator**

If the laser is operating in a stationary state, we can see that it is emitting several longitudinal modes. These are exactly the same modes that will be found in the emission profile. Since the modes are fed by an inhomogeneous emission profile they can also exist independently. The He-Ne-Laser is a classic example of this.

### 2.3 Resonators

In the following section some fundamentals used in the description and calculation of optical resonators will be introduced. Stability diagrams, the beam radius and beam sizes for the resonator types used in later experiments will be calculated and discussed. The investigations and calculations will be carried out for an "empty" resonator since the characteristics of the resonator will be particularly influenced (e.g. thermal lenses, abnormal refractive index etc.). The ABCD law will be introduced and used in this context. Just like the Jones matrix formalism this type of optical calculation is an elegant method of following the beam (ray tracing) in a complex optical system. Fig. 13 shows that an identical lens system can be constructed for every optical resonator. The beam path of the resonator can be traced using the ABCD law, aided by an equivalent lens system. So, how does the ABCD law work ?

First we must presume that the following calculations are correct for the limits of geometric optics, that is if the beam angle is < 15° to the optical axis, close to $\sin\alpha \cong \alpha$. This has been fulfilled in most systems, especially for laser resonators. A light beam is clearly defined by its height x to the optical axis and the slope at this
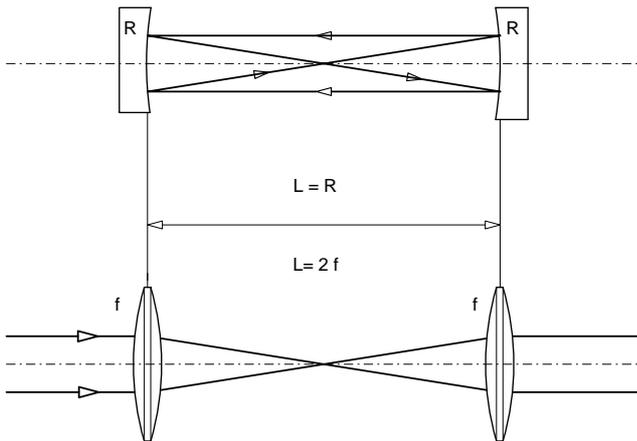


**Fig. 13: Spherical resonator with equivalent lens guide**

point (Fig. 14).
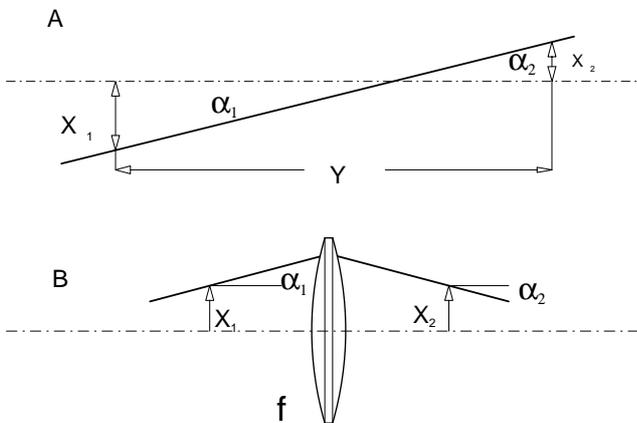


**Fig. 14: (A) light beam with the characteristic parameters, (B) Trace through a lens.**

The matrix to be introduced is called the beam transfer matrix or ABCD matrix. When this matrix is applied to the input quantities $x_1$ and $\alpha_1$ the resulting output quantities will be $x_2$ and $\alpha_2$:

$$\begin{pmatrix} x_2 \\ \alpha_2 \end{pmatrix} = \begin{pmatrix} A & B \\ C & D \end{pmatrix} \cdot \begin{pmatrix} x_1 \\ \alpha_1 \end{pmatrix}$$

Example A in Fig. 10 shows the free propagation of a beam, from which we can deduce that $\alpha_1 = \alpha_2$ and $x_2 = x_1 + \alpha_1 y$. So, the ABCD matrix in this case is:

$$A = \begin{pmatrix} 1 & y \\ 0 & 1 \end{pmatrix}$$

In example B which shows a thin lens the matrix is:

$$B = \begin{pmatrix} 1 & 0 \\ -1/f & 1 \end{pmatrix}$$

It is easy to understand that the combination of example A and B is a result of free beam propagation with subsequent focusing with a thin lens

$$X_2 = A \cdot B \cdot X_1$$

A series of ABCD matrices for different optical elements can be drawn out with this method. They have been compiled by Kogelnik and Li [3]. The above examples are sufficient for the calculation of a resonator. Beams in an optical resonator have to pass through the same optical structure several times. After passing through it n times the ABCD law for a particular place Z of the lens guide (Fig. 13) would be:

$$\begin{pmatrix} x_f \\ \alpha_f \end{pmatrix}^n = \begin{pmatrix} A & B \\ C & D \end{pmatrix}^n \cdot \begin{pmatrix} x_i \\ \alpha_i \end{pmatrix}$$

In this case the ABCD matrix is the identical lens guide given to the resonator. The n-th power of a 2 x 2 matrix is calculated as follows:

$$\begin{pmatrix} A & B \\ C & D \end{pmatrix}^n = \frac{1}{\sin(\theta)} \cdot \begin{pmatrix} a & b \\ c & d \end{pmatrix}$$

$$a = A \cdot \sin(n\theta) - \sin((n-1) \cdot \theta)$$

$$b = B \cdot \sin(n\theta)$$

$$c = C \cdot \sin(n\theta)$$

$$d = D \cdot \sin(n\theta) - \sin((n-1) \cdot \theta)$$

$$\theta = \arccos\left(\frac{A+D}{2}\right)$$

The trace of the above ABCD matrix |A+D| must be $\leq 1$ if the beams are to remain within the lens guide. So,

$$|A + D| \leq 1 \qquad \textbf{Eq. 2.5}$$

This is now the criteria of stability for the lens guide and therefore also for the accompanying resonator.

Let us conclude.

An identical lens guide system can be allocated to every resonator. The ABCD matrix is determined for this optical structure (several simple lenses). The stability diagram for the different mirror intervals with given mirror radii is deduced using Eq. 2.5.
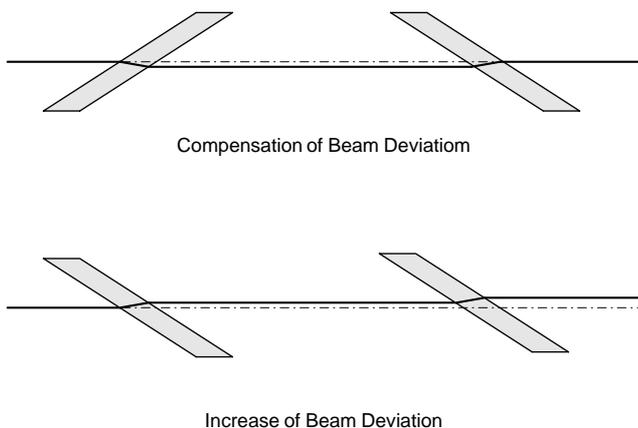
## 2.4  Laser tubes and Brewster windows

Brewster windows function in two ways. They hermetically seal the tube, as well as ensuring that there is a definite polarisation in laser oscillation without additional losses.
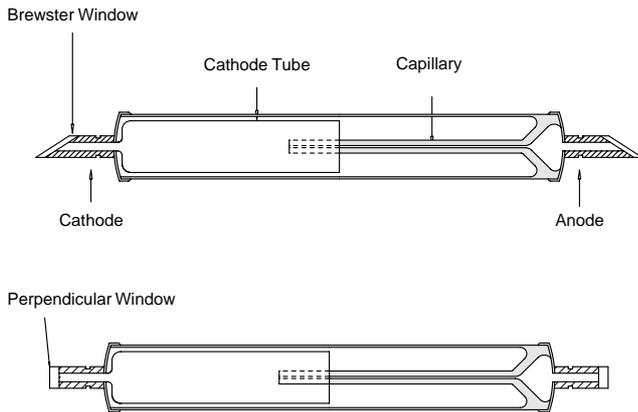


**Fig. 15: Laser tube with Brewster windows as used in the experiment and perpendicular windows with highly anti reflection coating**

The discharge only burns in the capillary. This is ensured by the expansion and melting of the capillary with the glass tube. Brewster windows are soldered on to a special metal (Vacon). The window flange on the anode side is made completely out of glass, to prevent coming into contact with the harmful high voltage during the required cleaning work. The tube being used has a ignition voltage of approx. 8 k V and an operating voltage of approx. 2 kV. The optimal current for the 632 nm line is 5 mA.



Compensation of Beam Deviatiom

Increase of Beam Deviation

**Fig. 15: Two possible arrangements of Brewster windows. The one above compensates for displaced beams.**

The Brewster windows of the laser tube are arranged in a way that enables compensation for beam displacement by the windows.

## 2.5  Wavelength selection

Lasers that are continuously variable from UV to IR, are probably the dream of every laser physicist. There has been a lot of research in this area and some goals have been partially achieved. e.g. The dye laser is a variable laser, but it is only variable at a wavelength of approx. 50 - 100 nm, depending on the dye used each time. The dye laser is being increasingly replaced by Titan -Sapphire lasers which emit from dark red to IR. A birefringent filter is usually used in these systems as a tuning element, as described in 2.5.2. Both lasers require argon-ion lasers as a source of pumped light. This laser can oscillate on several lines. The tuning element in this case is a Littrow prism, as described below.

### 2.5.1  Littrow prism

Littrow's idea is simple, therefore it is also ingenious. He produced a prism in which the refractive angle is measured in such a way that, in the arrangement of the minimal deviation (beam runs parallel to the hypotenuse), the beam enters the prism just under the Brewster angle. In this way, there are no reflection losses. This kind of prism is also known as a Brewster prism.

Littrow then took the prism apart by cutting it down the middle and coated the ensuing surface with a highly reflecting substance. If the refractive index of the first layer is similar to the prism material, the Fresnel losses will be considerably reduced and the result will be an element suffering few losses, that can be used inside the resonator to select wavelengths.



Arrangement within the Laser Resonator
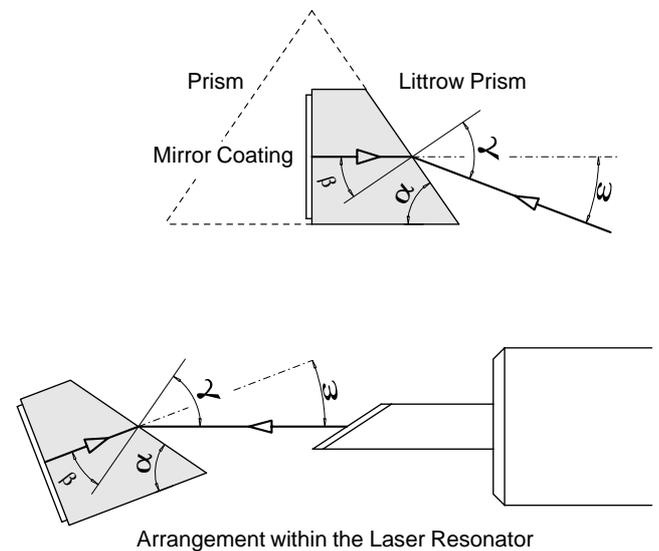
**Fig. 16: Formation of a Littrow prism out of a Brewster prism and its arrangement inside the resonator**

### 2.5.2  Birefringent crystal

Birefringent crystals are indispensable in laser technology. They are used as optical retarder and also as tuning elements. At this point we will introduce a formalism describing the interaction between light and birefringent optics in a simple way. This formalism enables us to analyse and represent the way in which various birefringent components work, with regard to computer applications in particular.

### 2.5.3  Jones Matrix Formalism

Jones created the basis for this formalism in 1941. We should really be grateful to him. He was probably one of those people who didn't think much of exercises with complex numbers and sin and cos theorems.

The electric field intensity of light is usually represented in the vectorial form:

$$\vec{E} = \vec{E}_0 \cdot \sin(\omega t + \vec{k}\vec{r} + \delta)$$

$\vec{E}_0$ is the amplitude unit vector describing the size and direction (polarisation) of the electrical field

$\omega = 2\,\pi\nu$ , $\nu$ is the frequency of light
t is the time

$\vec{k}$ is the wave vector, containing the propagation direction and the wavelength $\lambda$, $\left|\vec{k}\right| = \frac{2\pi}{\lambda}$

$\vec{r}$ is the displacement vector in the system of coordinates of the light wave

$\delta = \frac{2\pi}{\lambda}\left|\vec{r}_1 - \vec{r}_2\right|$ is a constant phase shift with respect either on a fixed coordinate or a fixed frequency

A complete description of a light wave still requires information on the magnetic field of the light wave. However, it need not be considered for most applications in the field of optics since the interaction of light with materials that do not absorb, is primarily of an electrical nature and not a magnetic one. As regards strictly theoretical derivations the magnetic field must fulfil certain conditions for continuity at the bordering surfaces. We do not propose to reflect on this aspect, however, and will therefore not discuss it any further at this point.
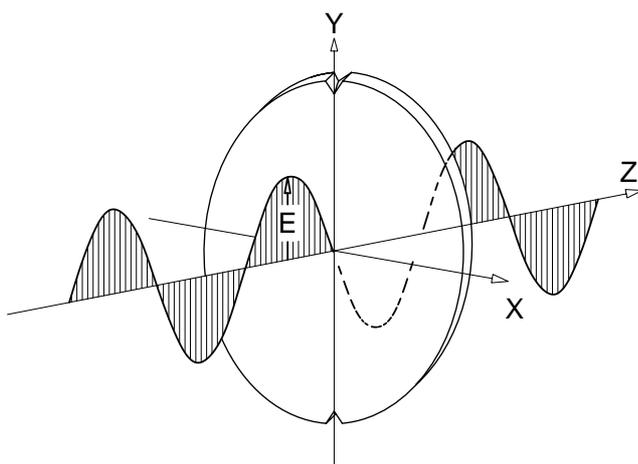


**Fig. 17: Passage of a light wave through an optical plate. The term "optical" is used to indicated that this plate has been manufactured for optical applications and that apart from characteristics specific to the material, the light wave has no outside obstacles (e.g. bubbles, impurities, etc.).**

The situation represented in Fig. 17 is typical for the use of birefringent components. It is therefore sufficient to be interested only in the X and Y components of the electrical field E. So, the light wave will be described by

$$J = \begin{pmatrix} E_x \cdot e^{i\omega t} \\ E_y \cdot e^{i\omega t + \delta} \end{pmatrix} \qquad \textbf{Eq. 2.6}$$

Since the frequency of the X and Y amplitude will always be the same and for power calculations fast oscillating terms will be neglected, we can simplify Eq. 2.6 to:

$$J = \begin{pmatrix} E_x \\ E_y \cdot e^{i\delta} \end{pmatrix}$$

Let us normalise the power P of the light wave to 1. Then

$$P = E_x^2 + E_y^2 = 1$$

It can easily be deduced that:

$$P = J\,J^{-1}$$

The minus sign in the J exponent means the conjugate complex of J (i.e. substitute i by -i). For a light wave that is polarised in the direction of the Y-axis it will be:

$$J = \frac{1}{\sqrt{2}} \cdot \begin{pmatrix} 0 \\ 1 \end{pmatrix}$$

In an analogous representation for a wave polarised in the direction of X the equation would be:

$$J = \frac{1}{\sqrt{2}} \cdot \begin{pmatrix} 1 \\ 0 \end{pmatrix}$$

We know that, based on the validity of the superposition principle of linear optics, any given number of polarised linear waves can be represented by the vectorial addition of two mutually perpendicular individual waves. By adding the two Jones vectors given above we would get linear polarisation of light oscillating at 45 degrees to the X or Y axis.

$$J = J_1 + J_2 = \frac{1}{\sqrt{2}}\begin{pmatrix} 1 \\ 0 \end{pmatrix} + \frac{1}{\sqrt{2}}\begin{pmatrix} 0 \\ 1 \end{pmatrix} = \frac{1}{\sqrt{2}}\begin{pmatrix} 1 \\ 1 \end{pmatrix}$$

If one component has a phase shift $\delta$ with respect to the other component, the result will be elliptical polarised light. If the phase shift $\delta$ is $\lambda/4$ the result will be the circular polarisation of light.

$$\delta = \frac{2\pi}{\lambda} \cdot \Delta \quad , \quad \Delta = \frac{\lambda}{4} \Rightarrow \delta = \frac{\pi}{2}$$

The Jones vector for this kind of light has the following form.

$$J = \frac{1}{\sqrt{2}} \cdot \begin{pmatrix} 1 \\ i \end{pmatrix} \quad note : e^{\frac{i\pi}{2}} = i$$

An optical component which can produce such a phase shift is called „ birefringent „ or double refractive. An element which works selectively on one component only works as polariser. The difference between the two is that whereas the polariser removes a component, the birefringent plate slows one component down in relation to the other, in a way that the components differ in phase behind the plate. Before giving the Jones matrices for these elements we will explain

briefly the way the elements work. A simple model will be used for this purpose. Light will be observed as an electromagnetic oscillation. We consider the optical component as a collection of many dipoles. These dipoles are determined by the type and form of the electron shells which each atom or molecule has. These dipoles are excited by the electromagnetic field of the light and are thus turned out of their equilibrium (susceptibility).The dipoles absorb energy of the light (virtual absorption) and send them out again. However, a dipole cannot send its beam in the direction of its own axis. If a crystal has two kind of dipoles, which are at a particular angle to each other, they can only emit and absorb light within the area of their angles. If the process of absorption and emission is slower in one kind of dipole than in the other there will be a phase shift. Macroscopically it seems as if there were a higher refractive index. A change in beam direction takes place because of the different dipole directions, i.e. there are two separate beam directions within the component. If a parallel light beam penetrates into this kind of material the result is, indeed, two beams leaving the crystal. In this case both beams are polarised perpendicularly to each other and have a phase shift between each other.
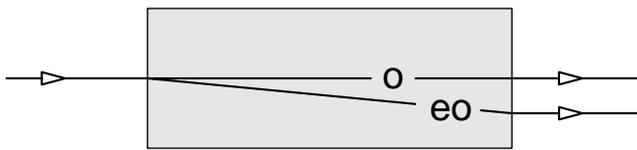


**Fig. 18: Birefringent crystal**

This phenomenon is called birefringence. These two marked directions of the crystal also have two distinctive refractive indices. Since one beam appears to be violating the Snell's law, it is called extraordinary (eo) and the one behaving normally is ordinary (o). Crystal quartz and calcite are materials which behave in this way. There are also a series of other crystals but these two have proved successful in laser technology. Thin plates, used as optical retarder are mostly made out of quartz because it is hard enough for this purpose. Mica sheets have also been used but they are not suitable for use inside the resonator because of the losses involved. Please note that only crystal quartz has a birefringent behaviour. Quartz that has already been melted (Quartz glass) loses this quality. A whole series of laser components are made out of calcite [1]. Short calcite crystals are sufficient to produce the required beam separation, e.g. as with the active Q-switch, because of the great difference between the ordinary and extraordinary refractive indices. The Jones matrix formalism can now be applied in the description of the interaction of a light wave with such materials. Retarding plates and polarisers can be represented as Jones matrices in the same way that a plane wave can be represented as a Jones vector. Polarisers which allow X or Y polarised to pass are as follows:

$$P_x = \begin{pmatrix} 1 & 0 \\ 0 & 0 \end{pmatrix} \text{ and } P_y = \begin{pmatrix} 0 & 0 \\ 0 & 1 \end{pmatrix}$$

If the polariser is turned around the beam over the angle θ, P must be treated with the transformation or rotational matrix:

$$R(\theta) = \begin{pmatrix} \cos(\theta) & \sin(\theta) \\ -\sin(\theta) & \cos(\theta) \end{pmatrix}$$

and the result for the turned polariser will be:

$$P(\theta) = R(-\theta) \cdot P \cdot R(\theta)$$

A birefringent plate whose optical axis runs parallel to the x or y axis has the following Jones matrix:

$$V = \begin{pmatrix} e^{-i\frac{\delta}{2}} & 0 \\ 0 & e^{i\frac{\delta}{2}} \end{pmatrix}$$

and has also to be transformed by the rotational matrix R(θ) in case the optical axis of the crystal was rotated around the angle θ. To prevent misunderstandings regarding the optical axes, we must point out that the optical axis of the crystal is the one in which the ordinary refractive index is effective. An account of an examination carried out with a λ/2 plate using the Jones matrix formalism is given in [1]. A birefringent plate made out of crystal quartz is used in the He-Ne experimental laser for selecting the wavelengths. This kind of element is also known as a birefringent filter or birefringent tuner. This element was originally used to tune dye lasers. It was first successfully used in a He-Ne laser by this author [2]. The arrangement within the laser is shown in Fig. 19.
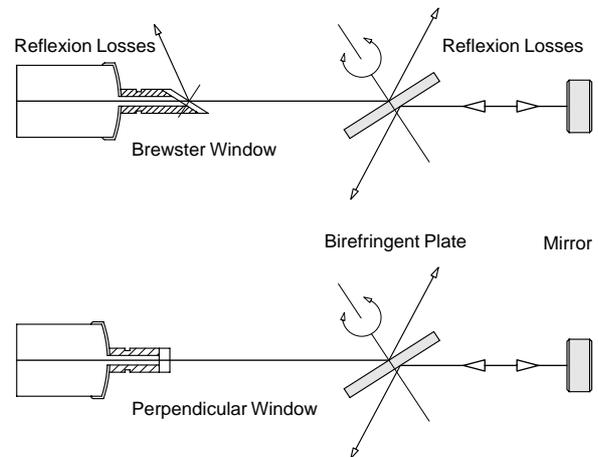


**Fig. 19: Birefringent filter for wavelength selection in-side the resonator**

The birefringent plate is placed under the Brewster angle into the resonator of the He-Ne laser to avoid reflection losses through the plate itself. The laser can only oscillate in a direction of polarisation given by the Brewster window or in case of the use of perpendicular windows in the direction of polarisation given by the birefringent plate itself. The birefringent plate does not change the polarisation if a phase shift of $\delta = 2\pi$ occurs between the ordinary and extraordinary beam after passing through it twice. In this case there will be no reflection losses at any plate orientated under the Brewster angle. The polarisation of the returning wave changes at every other value of the phase shift $\delta$ and there are reflection losses at the Brewster window where the laser will stop oscillating. The phase shift caused by the

plate is calculated as follows. The optical path of the ordinary beam is

$$l_o = d \cdot n_o$$

The path of the extraordinary beam is

$$l_{eo} = d \cdot n_{eo} \text{, so}$$

$$l_o - l_{eo} = d \cdot (n_o - n_{eo})$$

the phase shift $\delta$ is :

$$\delta(\theta) = \frac{2\pi}{\lambda} \cdot 2 \cdot d \cdot (n_o - n_{eo}(\theta))$$

after passing through twice, where d is the geometric path followed by the beam in the plate with thickness $D$ and $\theta$ is the angle between the electric field vector of light and the optical axis of the crystal lying in the plane of the plate. When

$$\delta(\theta) = \frac{2\pi}{\lambda} \cdot 2 \cdot d \cdot (n_o - n_{eo}(\theta)) = 2\pi$$

there are no losses at the Brewster window. This applies to a given wavelength for a particular angle $\theta$. Now, the thickness $D$ and the rotational angle $\theta$ of a plate must be determined using the Jones matrix formalism and which fulfil the above condition in the wavelength area of visible and infrared beams of the He-Ne laser.
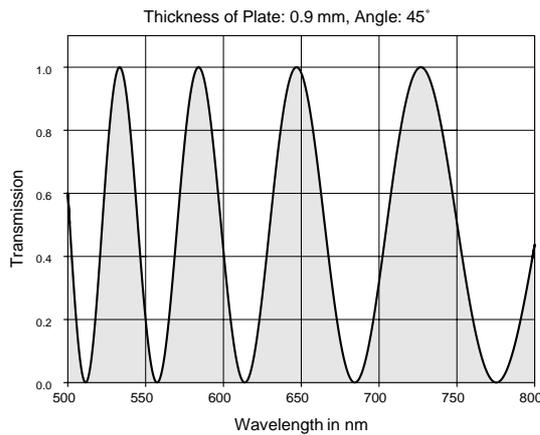


Fig. 20: **Transmission of a BFT with a plate thickness of 0.9 mm, an angle of 45⁰ between the electrical field vector and the optical axis calculated for a wavelength range of 500 - 800 nm**

The dispersion of the birefringent quartz was taken into account in this case. This is why the transmission curves change to higher wavelengths.
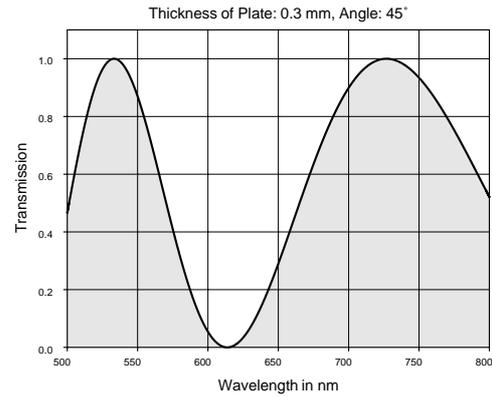


Fig. 21: **The same calculation as in Fig. 20 but with a plate thickness of 0.3 mm. The thinner the plates are, the wider the transmission curves**
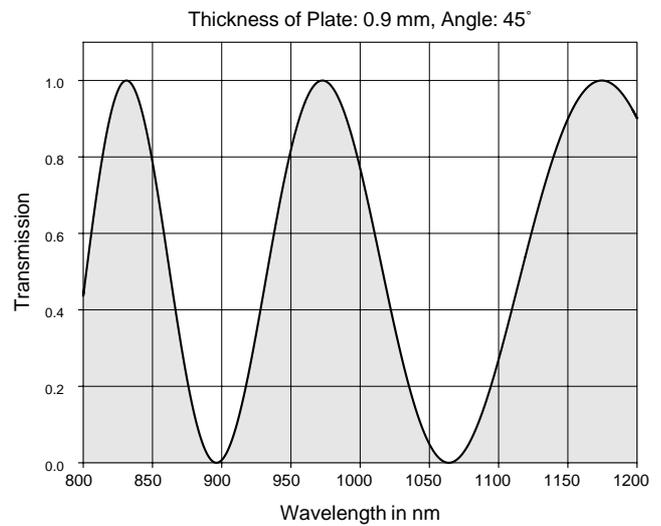


Fig. 22: **Calculation as in Fig. 20 but with a wavelength range of 800 - 1200 nm. The transmission curves are wider because of the dispersion.**
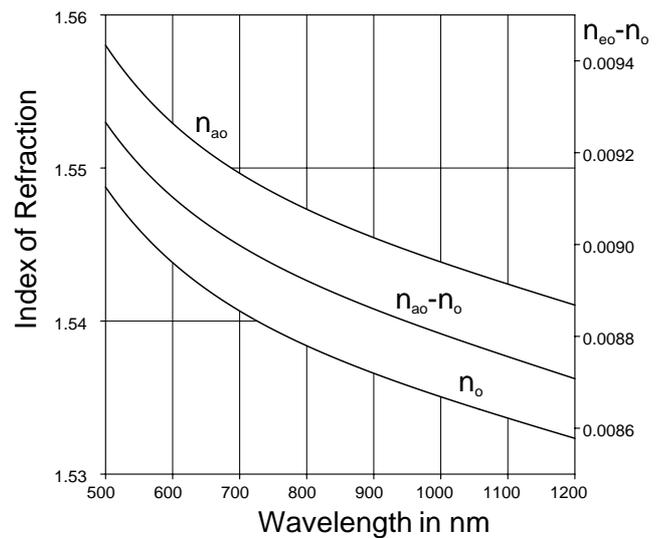


Fig. 23: **Dispersion curve for the ordinary and extraordinary refractive index**

## 2.6 Mode selection

In some areas such as high resolution spectroscopy or interferometric measuring techniques several modes in the laser light prove to be very disturbing. (coherent length). Selective frequency losses can be brought into the resonator by an etalon and undesirable modes are damped and suppressed in this way.

An etalon is a plane parallel, low quality resonator. The etalon usually consists of an individual glass body whose plane surfaces are well ground and polished, parallel to each other.

Just like a normal resonator, an etalon also has modes. However, its modes are considerably broader since the reflection on the plane surfaces is kept low
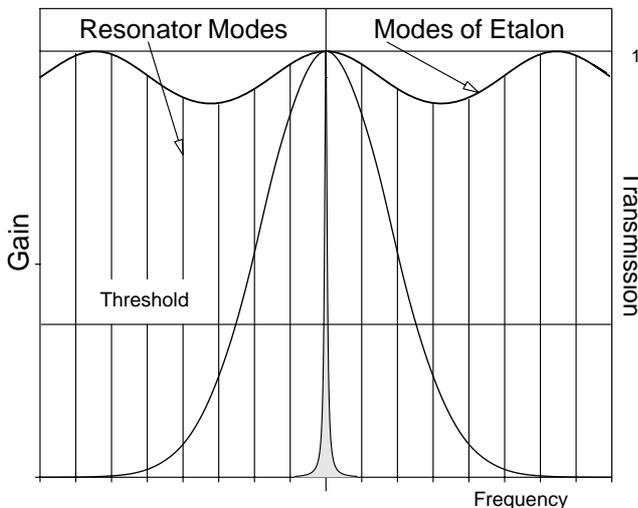


**Fig. 24: Mode selection with an etalon**

If the etalon is tilted by the angle $\gamma$ against the incoming beam the maximum transmission will change according to:

$$\lambda_m(T = 1) = \frac{2 \cdot d}{m} \cdot \sqrt{n^2 - \sin(\gamma)} \qquad \textbf{Eq. 2.7}$$

In this case m is the m-th order, d the thickness of the etalon, n is the refractive index and $\gamma$ the tilt angle.

According to Eq. 2.7 the etalon modes can be shifted by tilting the etalon while of course the amplification profile and the resonator modes stay the same. In this way it is possible to encounter more losses in modes that oscillate due to the threshold value amplification than in modes lying just below the maximum transmission.

As in the case of a simple resonator, the distance between the modes is given by the thickness d and the refractive index n:

$$\Delta v = \frac{c}{2nd}$$

The etalon must be designed according to the degree of suppression imposed on neighbouring modes and the spectral distance between them. In the HeNe experimental laser used in the following experiments the etalon is 1 cm thick and does not have any additional coating but only 4% reflection on each side due to the Fresnel losses.

## 2.7 Bibliography

(1) **B.Struve, W.Luhs, G.Litfin,** Crystal optics and its importance in laser technology, Year book for optics and precision mechanics 1989

(2) **W.Luhs, B.Struve, G.Litfin,** Tuneable multi lines He-Ne laser, Laser and optoelectronics, 4. 1986, AT-Fachverlag GmbH Stuttgart

(3) **Kogelnik and Li**

# 3 Experiment

The experiments start with adjusting the basic set up. This is described in the appendix from page 1 onwards. Once the basic adjusting has been done (see up to page 5 of the appendix), we can begin the first experiment.

## 3.1 Optical stability

The optical resonator of the He-Ne laser is designed according to the given active material (Ne) and the required beam quality.

The objective is to achieve the best possible beam output in the basic Gaussian mode (TEM$_{00}$).

Generally speaking these are two contradictory requirements since a high power output requires the use of a large volume of the active material, whereas the fundamental mode is restricted to its own volume.

This is why the hemispherical resonator has the optimal configuration for the He-Ne laser.

## 3.2 Gaussian beams

This can be explained by the characteristics of Gaussian beams. The beam radius w (w = waist) is a result of the following relationship:

$$w(z) = w_0 \cdot \sqrt{1 + \left(\frac{z}{z_R}\right)^2}$$

$w_0$ is the smallest beam radius at the minimum of the beam waist and $z_R$ is the Rayleigh length.

$$z_R = \pi \cdot \frac{w_0^2}{\lambda}$$

Fig. 25 shows the relationship between the beam diameter and the length z. z points into the direction in which the beam is propagating.
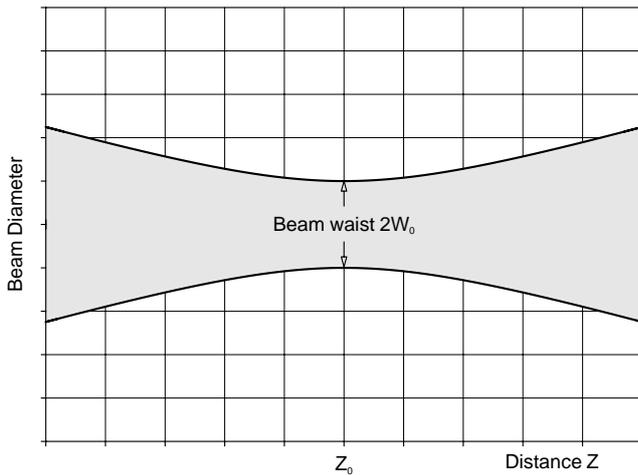
**Fig. 25 The beam diameter of a Gaussian beam in the fundamental mode**

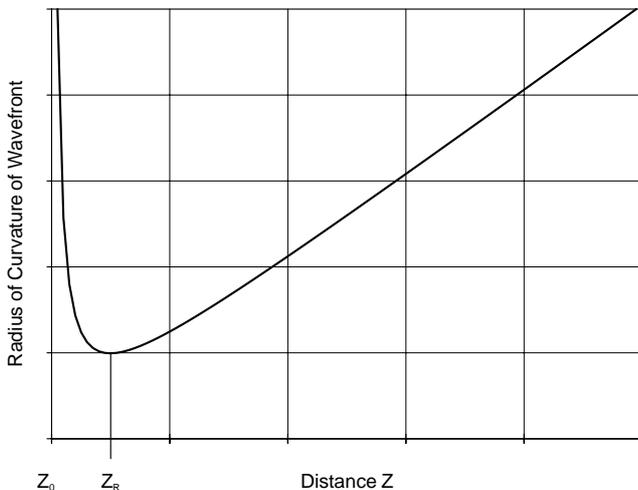The beam's radius is smallest at the location $z_0$. The beam radius increases in a linear form as the distance increases. Since light waves are spherical waves a radius of curvature of the wave front can be allocated to each location z. The radius of curvature $R(z)$ can be calculated with the following relationship:

$$R(z) = z + \frac{z_R^2}{z}$$

This is illustrated in Fig. 26



**Fig. 26: Radius of curvature of the wave front versus the distance z from the beam waist at z=0**

At $z = z_R$ the radius of curvature is at a minimum and increases at l/z against zero. The radius of curvature at z=0 is infinite. At this point the wave front is plane.

Above the Rayleigh length $z_R$ the radius again increases in linear fashion. This is a basic but important statement. It shows that there is a real parallel beam at only one point of the light wave, that is at its focal point. In the range

$$-z_R \leq z \leq z_R$$

a beam can be considered as parallel or collimated. Fig. 27 shows the Rayleigh range as well as the divergence θ in the far field.
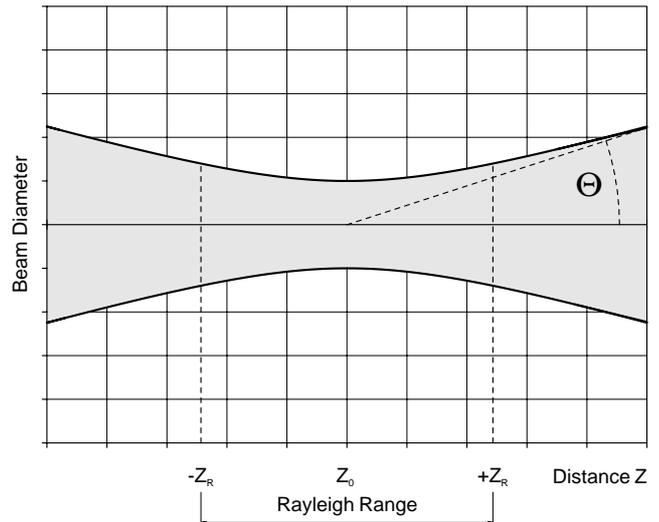


**Fig. 27: Rayleigh range and divergence**

When reversing the operation a stable optical resonator can now be constructed by adapting the radii of curvature in such a way that they correspond to the radii of curvature of the basic Gaussian mode. This is shown in Fig. 28.
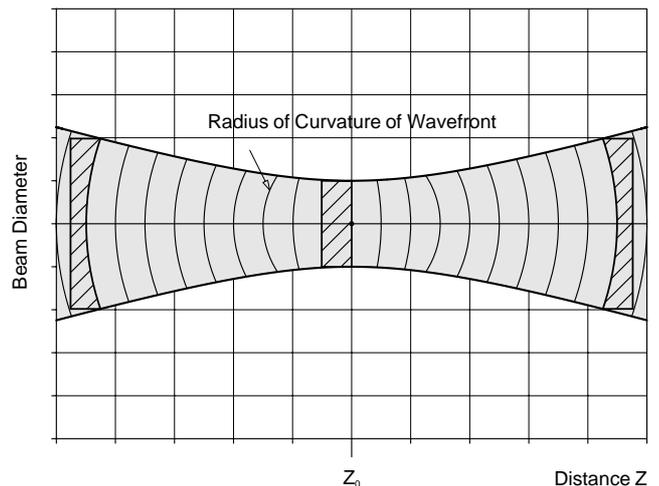


**Fig. 28: Construction of an optical resonator with mirrors. The resonator has the same radii of curvature as the fundamental Gaussian mode has at particular points of z**

Fig. 28 shows a spherical and a hemispherical resonator. If a laser is made to oscillate with this kind of configuration the beam path can be calculated with the above mentioned equations based on the knowledge of the mirror radii and the distance between the mirrors. Due to the demand for a high output power in the fundamental mode, a spherical arrangement is out of question for the He-Ne laser. Transversal modes can also oscillate in spherical resonators. This could also be achieved in this type of resonator by putting up a diaphragm inside the resonator which only allow the fundamental mode to pass freely. However, this option is complicated. The hemispherical resonator is chosen because the place of the plane wave front is very well defined. Only the fundamental mode is reflected back with low losses. Moreover, the He-Ne laser requires a narrow capillary (Chapter 2.1). The recombination process

of the laser cycle takes place on its walls. As far as the active material is concerned, the diameter of the capillary should be as small as possible to enable an optimal laser output, but it should not be so small as to block the path of the fundamental mode. The course the beam radius of the mode takes is determined by the radii of curvature and the distance between the mirrors. However, the mode volume, i.e. the volume filling up the fundamental mode, or the length of the amplifying material should be as large as possible to get as much output as possible from the active material. Long tubes are therefore used in He-Ne lasers to increase the output power. At the same time, the radius of the spherical mirror should be big enough for this purpose.

### 3.2.1  Measurements

The objective of the following experiment is the measurement of:
(1) The optical stability range
(2) The optical output as a function of the position of the laser tube inside the resonator
(3) The measurement of the beam radii path inside the resonator.

The measurement (1) will be carried out while the position of the spherical mirror during laser operation is changed up to the stability limit. It can be shifted by slightly loosening the fixing screw on the mirror adjustment support and is still resting lightly on the optical rail. Be careful that the laser oscillation does not break off due to the shift. The adjustment support is fixed into the new position again and the laser output brought to a maximum by readjustment. Carry on with this until you finally find a position in which no more laser oscillation can be achieved. This position is compared to the maximum distance L of the mirrors with the radius of curvature R which can be deduced from the following criteria of stability (see also Eq. 2.5):

$$-1 \le g_1 \cdot g_2 \le 1$$
$$g_1 = 1 - \frac{L}{R_1} \text{ and } g_2 = 1 - \frac{L}{R_2}$$

The measurement of the output power (2) as a function of the position of the laser tube (capillaries) in the resonator is carried out by loosening the fixing screw on the larger carrier which holds the tube and whose position will be changed. Straight after the first adjustment has been made, it should be ensured that the mechanical axis of the tube corresponds to the optical axis which is defined by the pilot laser. you will see that the laser output decreases when the position of the tube is brought closer to the spherical mirror. The discussion of the result is based on the beam radius path of the resonator used in consideration of a given capillary diameter. The beam radius path is then measured within the resonator at an optimal position of the laser tube. To measure the beam diameter at a particular position a calliper gauge is used as a measuring diaphragm. The calliper gauge

is adjusted to approx. 1.5 mm and placed in the beam path. It is moved back and forth and we then observe whether the laser oscillation returns or not. If it does, the value on the adjusted "diaphragm" is reduced till the laser does not light up any more. The last value at which laser operation was observed is read from the calliper gauge and noted down. This value is the beam diameter at that point. These measurements are repeated at different points and a diagram similar to Fig. 28 should be drawn. Repeat the measurements again but with a clearly changed position of the spherical mirror. Discuss the results taking the thoughts on the path of a Gaussian beam into consideration.

### 3.3  Output power

After carrying out the optimising of the optomechanic set-up in the last experiment, we will now measure the influence of the discharge current on the laser output. The output is measured with a photo detector for this purpose. Observe that fluorescent light is also caught by the detector during the discharge. This background must be taken into consideration since only mirrors that decouple very slightly are used for safety reasons. The background is taken with a very slightly de-adjusted resonator to avoid the occurrence of any laser oscillation. The measured background values are subtracted from the following measurement for the different currents in each case. The first series of measurements occurs at the "red line". After finishing the experiments the same measurements should be repeated for other wavelengths. The dependency found will be discussed in connection with the laser cycle. The desired population of the laser output level and the undesirable population of the laser terminating level play an important role in this case.

### 3.4  Mode structure

Using a lens with a short focal distance (approx. 30-50 mm) the laser's output beam is broadened and mapped on to a screen. The spherical set up of the resonator is used to represent the transverse modes. Higher modes will only be observed by slight de-adjustment. If this does not succeed transverse modes can also be forced. A known characteristic of higher modes is that they have areas where the electric field intensity of light is zero. A "short circuit" of this kind can also be achieved by inserting a thin wire ( even a strand of human hair will do) into the laser beam within the resonator. We can then see a separated distribution of intensities on the screen which look like transverse modes.

### 3.5  Wavelength selection

Wavelength selection is necessary for two reasons. The laser either has undesirable wavelengths due to its specific characteristics or it suppresses wavelengths which only oscillate when a certain wavelength does not oscillate. The latter is true of the visible lines and a part of the infrared lines of the He-Ne laser. Since the visible lines all start from the same level these lines compete with each other. The line with the lowest threshold oscillates first and uses the inversion for its own purposes. Wavelengths with different components can be selected. They are listed below.

### 3.5.1  Dispersive elements (prisms).

They do not suffer great losses. The separation of lines occurs in two ways. One is through dispersion and the other through geometric length, which is still feasible when carried out between the prism and the laser mirror belonging to it. If the lines are wide apart (approx. 20-30 nm), then distances of 5-10 mm (Littrow prism) are enough for the separation to occur. Lines lying closer together can be separated by a series connection of several prisms. In this procedure a lot of time has to be taken in adjusting, unless an adjustment laser of the same wavelength is available. Due to the Fresnel losses on the surfaces the laser system must have sufficient gain reserves.

### 3.5.2  Diffractive elements

(Grating). They deviate light in different order with respect to the wavelength. So called Blaze gratings are made in such a way, that the major part of the light is diffracted into the first order. However, the losses for a He-Ne laser are too big.

### 3.5.3  Interfering elements

(Fabry Perot or etalon, interfering filters). These elements can have very narrow bands but require pre-selected light since their transmission is repeated periodically. Interference filters seldom reach transmissions of more than 95 %. Etalons are used if modes have to be selected. The etalon itself only has the necessary tuning precision when combined with laser and resonator characteristics.

### 3.5.4  Elements sensitive to polarisation

(Lyot filter, birefringent filter). Birefringent filters (birefringent tuners) are always used when the laser or the line to be selected has a defined polarisation (e.g. Brewster surface). If they are put into use under the Brewster angle they will not suffer great losses. They have periodic transmissions, according to their thickness and wavelength range. They can separate lines lying close to each other without causing any important change in beam direction.

### 3.5.5  Littrow prism

The basic adjustment is explained from page 24 chapter 4.3 onwards. The Littrow prism is used instead of the plane laser mirror and it fulfils two requirements. It works as a prism for wavelength separation and as a plane laser mirror. Strictly speaking it should be possible to select all the lines of the He-Ne laser for which the coating of the surface of the Littrow prism is suitable. The lines are tuned by tilting the prism. In case the coated surface of the prism directly vertical to the optical axis of the resonator corresponds to the expected laser oscillation the line selected should also oscillate. In fact, this is not the case. We can observe that the dominant "red line" is still oscillating in spite of tilting the prism. However the beam path in the resonator changes (we can observe this at the spherical mirror). The laser beam wanders in the resonator as well, so in spite of the increasing losses, the amplification of the dominant line is sufficient and the others will not be made to oscillate. "Beam walking", an adjustment procedure in which the beam position in the resonator is changed, can be used to push the dominant line to such an extent on the edge of the possible oscillations that the orange line starts oscillating by further tilting of the LPT. "Beam walking" is carried out by slightly turning an adjustment screw on the laser mirror adjustment support and readjusting the output to a maximum by turning the opposite adjustment support in the same direction (x or y). Now the beam changes its direction in the resonator. The iris effect of the capillary stops it from going too far. The objective of the experiment is to understand wave selection with a prism, on the one hand and to get to know the concept of "beam walking" on the other.

### 3.5.6  Birefringent crystal

From page 22 chapter 4.1 onwards of the appendix the basic adjustment of the laser with a birefringent tuner (BFT) is explained. The BFT must be set up in the resonator at a place where the laser beam is parallel "as far as possible". The points made on the selective effect of BFT on page 9 were based on observations made on collimated beams. If this is not, there would be different angles to the optical axis in the area of a divergent beam. This leads to different phase shifts within the laser beam and thus to a blurring of the polarisation direction. However these effects are comparatively low. Additional losses could therefore be formed for the weak lines, which can be minimised by the optimal position of the BFT within the resonator. If no oscillation of the weak lines can be achieved, the following points must be checked and changed accordingly. All optical surfaces including the surface of the BFT must be well cleaned. The BFT must be adjusted to the Brewster angle to the optical axis. The discharged current should not be more than 5 mA.

### 3.6  Single mode operation with Etalon

The etalon used is a highly precise quartz glass body produced in a parallel fashion. The thickness is 10 mm and the surfaces are not coated. The etalon is mounted in an adjustment support and can be tilted perpendicularly to the axis of the resonator. The etalon is placed into the well adjusted resonator. Estimating at sight, the etalon is adjusted vertically. After placing the etalon into the resonator the laser should oscillate again. The etalon is now adjusted to the extent that it is vertical to the laser beam. We can observe this in the return reflections of the etalon and in the increased laser output. Now the etalon is at the zero order. By tilting it either horizontally or vertically the laser oscillation is stopped at first and starts oscillating at a particular tilt of the etalon. The first order m=1 has been reached. By tilting the etalon even further higher orders are reached. The output for every arrangement is measured and the result is discussed with reference to the so called "walk off" losses. If a Fabry Perot is available for analysis the single mode operation can be examined. The continuous tuning of the He-Ne laser within its amplification profile will also be observed. The variation in amplitude of the mode while tuning (slight tilting of the etalon) gives you the envelope of the gain profile of Ne.

### 3.7 *Operation with infrared lines*

**Note:** Operation with infrared lines is only possible when your system is equipped with a laser tube with Brewster windows. Tubes with perpendicular windows do have an anti reflection coating which is optimised for visible lines only.

The laser mirrors used till now are exchanged for IR mirrors in this experiment. The adjustment is analogous to the basic adjustment when operating with visible lines. Since infrared mirrors have a high transmission for the pilot laser, the return reflexes for adjustment are less, so the room must be slightly darkened when undertaking the initial adjustment. The laser oscillation is first observed with a IR-converter screen. The visible fluorescent beam is suppressed with a RG1000 coloured glass filter. The measurements are now carried out analogous to the measurements done to the visible lines. However the Littrow prism cannot be used in wavelength selection since it is only coated for the visible range. The attribution of the BFT selected lines should favourably be done with a monochromator.

## 4 Unpacking

The system comes packed in two storage and transportation boxes. Box one of two contains the components as shown below.
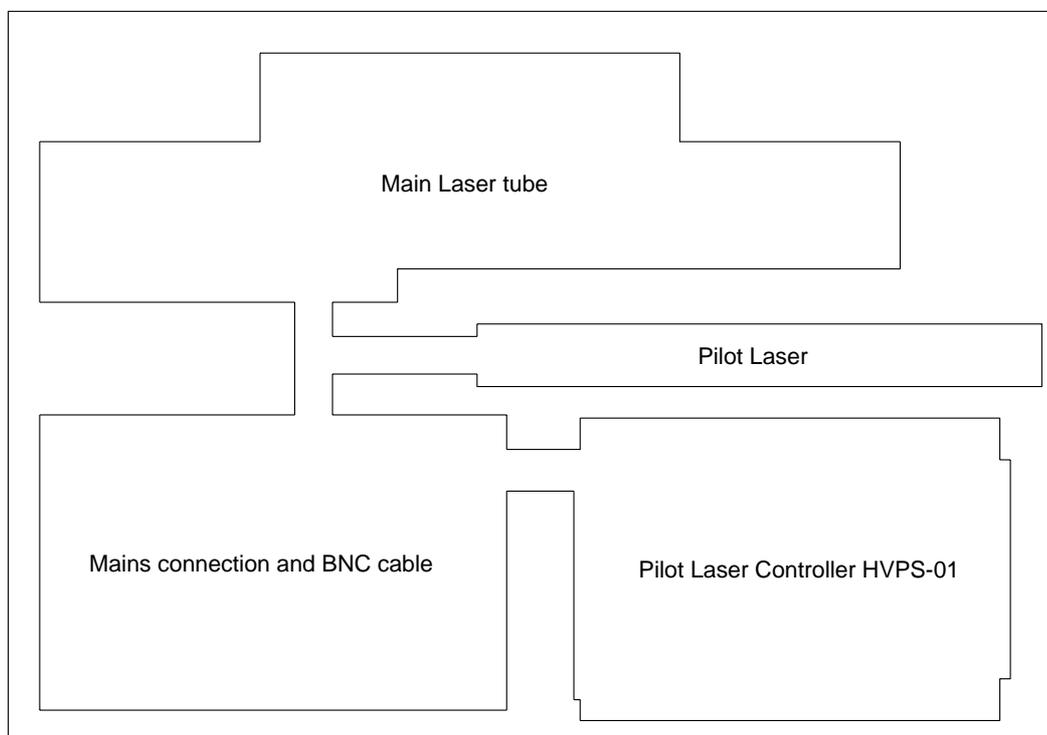


Foam padding of the box one of two and its content

The main laser tube must be connected to the tube controller TC-01 by means of the high voltage connector. It is recommended first to place the main laser tube onto the optical rail. Place the controller on to the desktop and connect the tube to the high voltage jacket on the rear of the tube controller TC-01. Since the connector is supplied with a safety interlock switch the system may not work until the connector is firmly inserted into the jacket. After this the controller maybe connected to the mains power, not before!
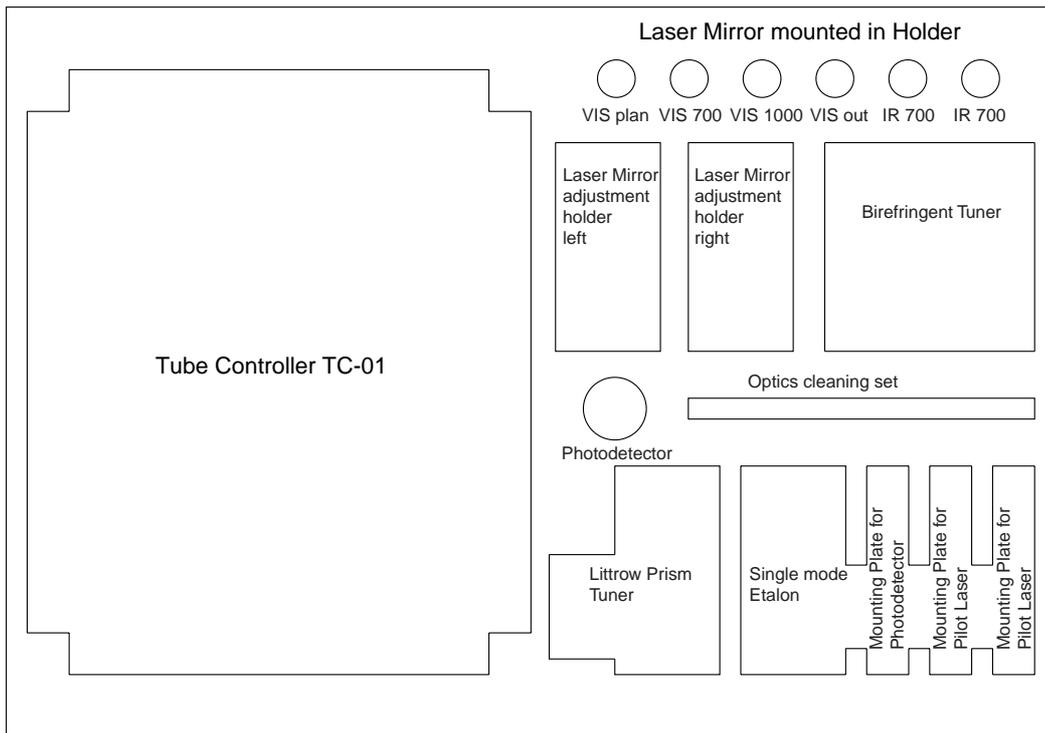
Depending on the actually ordered system the second box contains the above shown components.

# 5 Set-Up and Components used
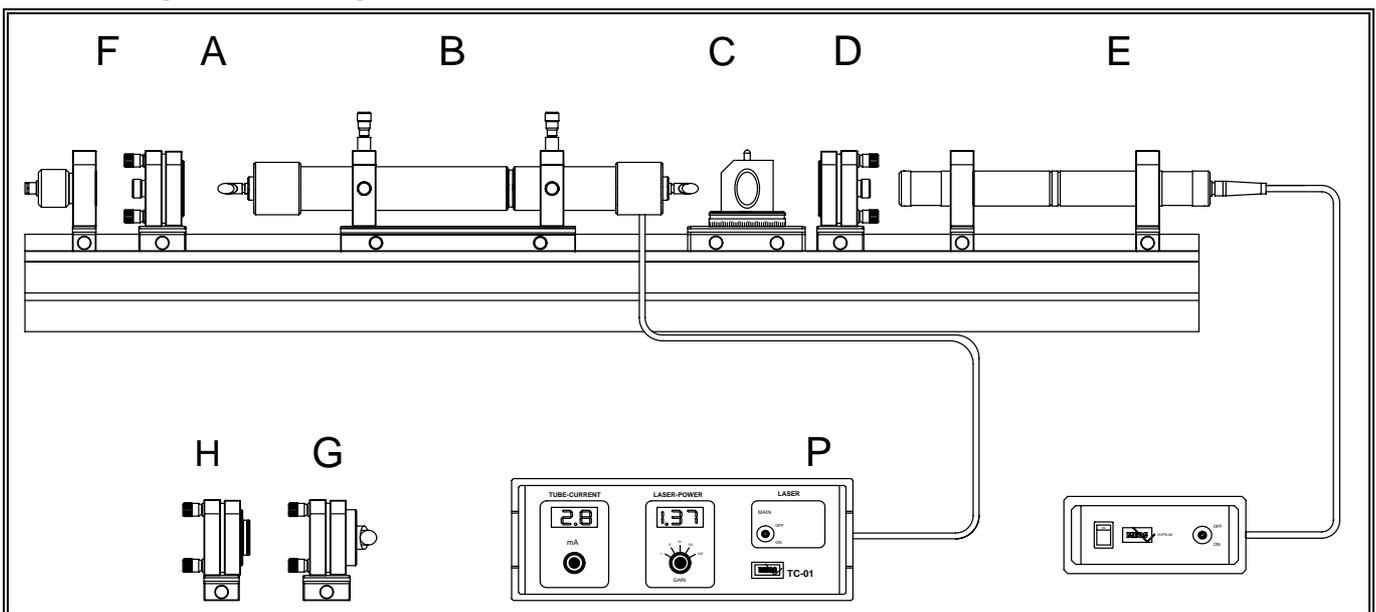


## Module A: Left laser mirror holder



This module contains the one resonator mirror (2). It can be screwed out with its fixture (1) from the holder (3). The mirror has a diameter of 1/2 inch and the experiment is supplied with a set of different mirrors.

## Module B: Main laser



HeNe-Laser tube with vertical windows on both sides mounted in two XY-adjustment holders on a carrier of 200 mm width. The windows are supplied with an high quality anti reflex coating. Anode and cathode are properly insu-

lated and „touch"-safe. Module B is firmly connected to the controller unit P. The anode of the main laser module is supplied with a voltage of up to 1500 V. Although the metal parts of the laser anode are insulated, cleaning of the laser window should only be done when the tube controller is switched off. Wait for 5 minutes before starting the cleaning process. If the tube is cleaned once before starting the experiments, it is sufficient for several hours

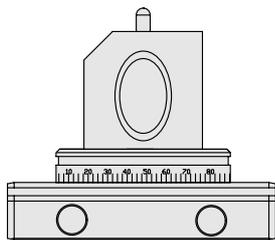### Module D: Right laser mirror holder

This module contains the one resonator mirror (2). It can be screwed out with its fixture (1) from the holder (3). The mirror has a diameter of 1/2 inch and the experiment is supplied with a set of different mirrors.

### Module C: Birefringent tuner

A plate of natural birefringent quartz is mounted in an rotator which allows the turning of the plate for tuning different lines of the main laser. With an additional rotator the plate can be tuned precisely to the Brewster's angle.

### Module G: Littrow prism tuner

A high quality BK7 Littrow prism is supplied with a high reflectivity (>99,98 %) coating in the range from 580 to 650 nm.
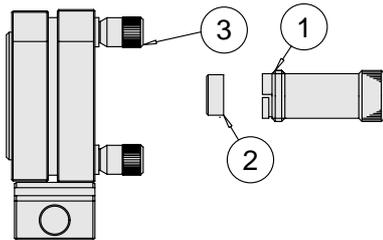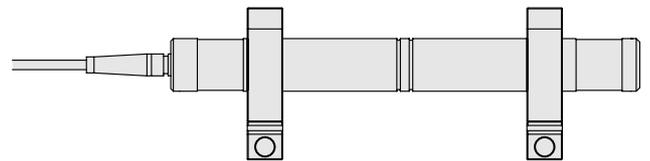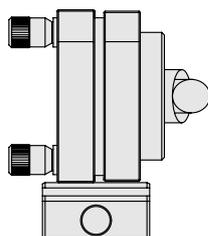
### Module H: Fabry Perot etalon
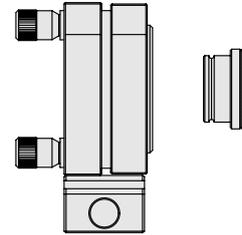
Single mode Etalon in „click"-mount with adjustment holder on carrier. The Etalon has a diameter of ½ inch and a length of 10 mm. No coating is provided, so that the finesse is determined by the Fresnell reflection losses.
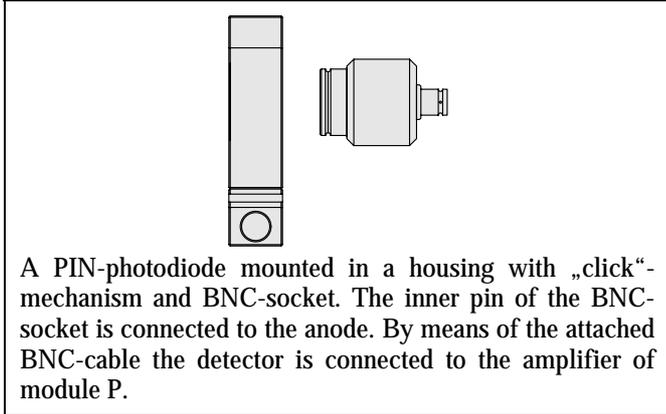
### Module E: Pilot laser

The pilot laser consists of an well centrally aligned HeNe-Laser mounted in mounting plates on carriers. The output power is 1 mW with random polarisation.

### Module F: Photodetektor



A PIN-photodiode mounted in a housing with „click"-mechanism and BNC-socket. The inner pin of the BNC-socket is connected to the anode. By means of the attached BNC-cable the detector is connected to the amplifier of module P.
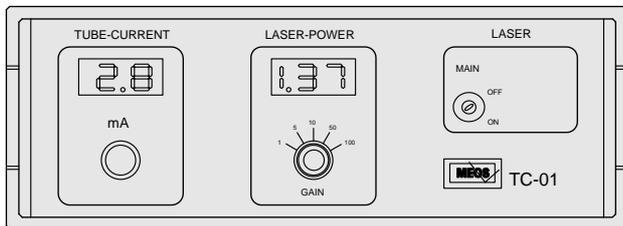
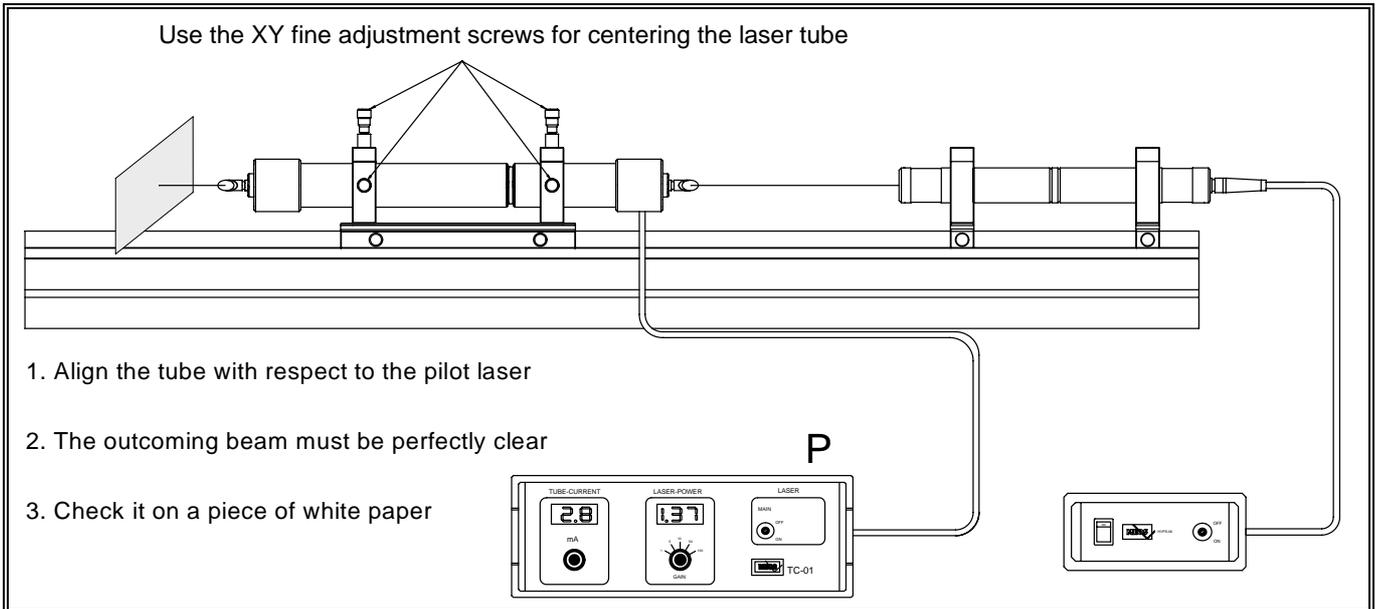### Module P: Tube controller



The controller unit TC-01 serves two purposes. It provides the high voltage for the main HeNe-Laser tube and contains a the photodiode amplifier for the measurement of the relative output power of the laser.

## *5.1 Basic alignment*



Use the XY fine adjustment screws for centering the laser tube

1. Align the tube with respect to the pilot laser

2. The outcoming beam must be perfectly clear

3. Check it on a piece of white paper

Place the pilot and main laser onto the rail and fix the clamps. Switch on the pilot laser while the main laser is switched off. The pilot laser is prealigned to the optical axis of the set-up and forms the optical axis of the main laser. Adjust the XY fine pitch screws of the tube holder so that the pilot laser beam passes the capillary of the He-Ne tube without any distortions.

Check the out coming beam by means of a piece of paper. Compare the spot on the paper with the spot of the incoming beam. They must be equal. The better this first tube alignment is, the easier you can put the main laser to oscillation.
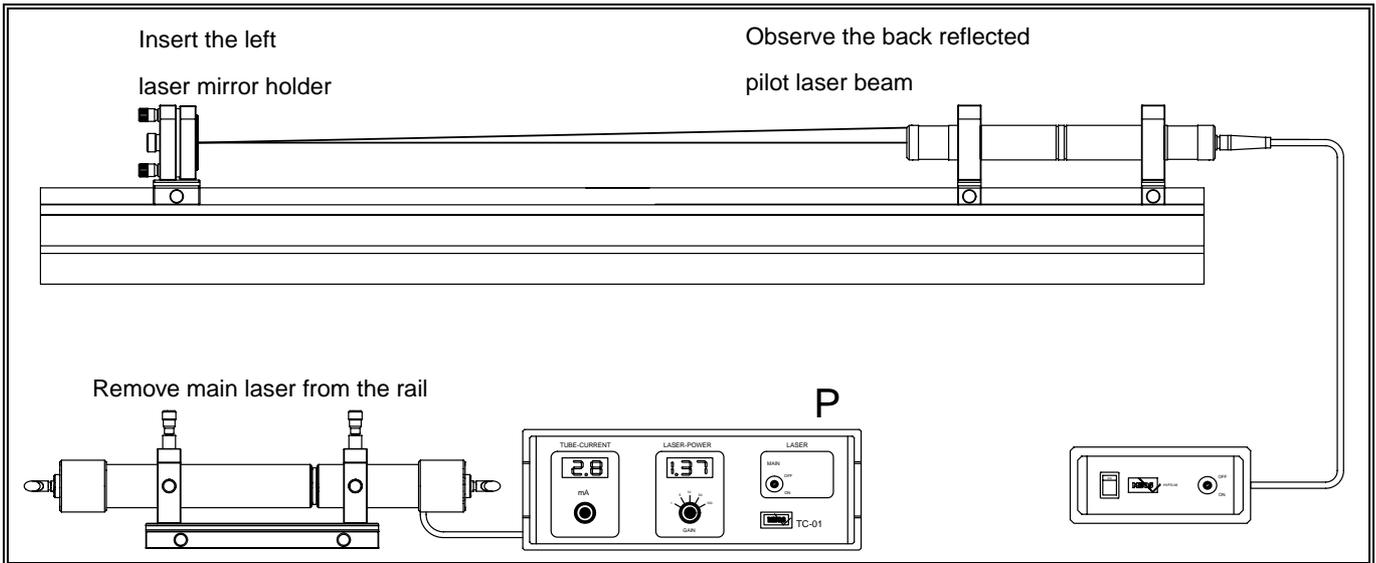
Place the laser mirror adjustment holder (the left one) onto the rail as shown in the above picture. Use the flat laser mirror with High reflectivity (VIS-PLAN) and screw it into the holder. Remove the aligned main laser module from the rail. Align the laser mirror in such a way that the reflected laser beam enters exactly the tube of the pilot laser. Observe the back reflected beam on the exit aperture of the pilot laser. When the reflected beam is aligned you will observe a flickering of the pilot laser intensity and interference fringes around the first spot. When the flat laser mirror is well aligned it forms with the resonator of the pilot laser a secondary resonator and interference effects are changing the intensity of the pilot laser beam. This is a hint that the first laser mirror is properly aligned with respect to the optical axis of the pilot laser.
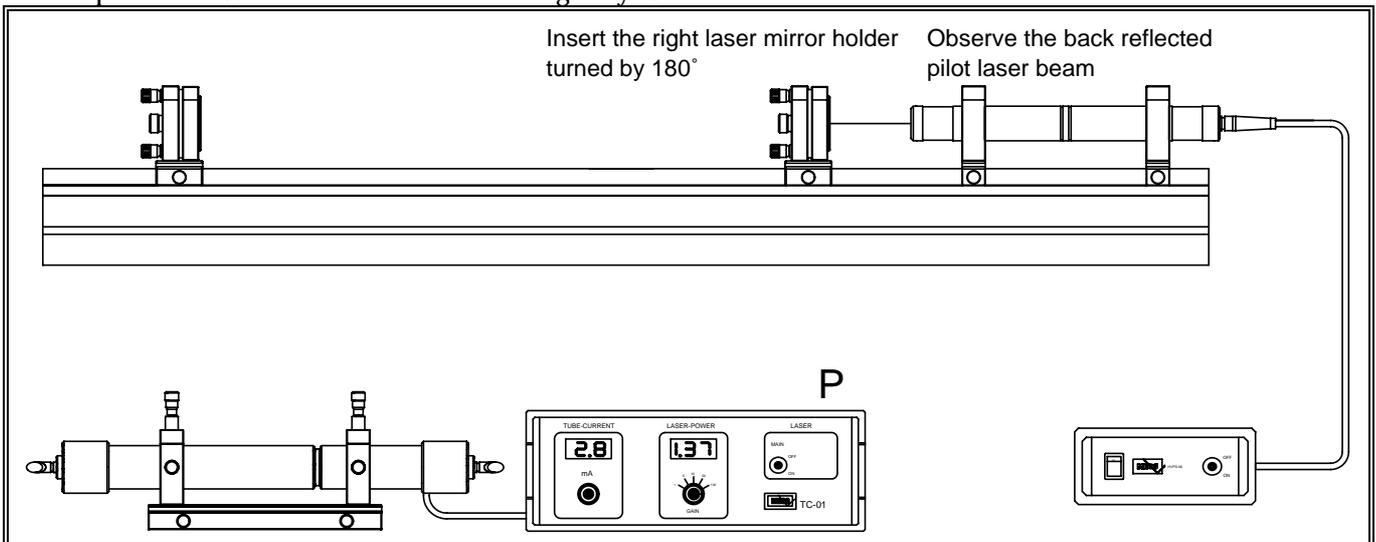


In the next step the second laser mirror adjustment holder is placed onto the rail as shown above. Use as second resonator mirror that one with the high reflectivity and a radius of curvature of 1000 mm (VIS1000). Place the mirror holder app. 600 mm apart from the first one. Because the mirror is a curved one, the back reflected light has a certain divergence. Adjust the back reflected beam so that it passes the exit aperture of the pilot laser beam. The nearer you adjust to the proper position, the more "laser beams " will occur all with increasing divergence. Centre 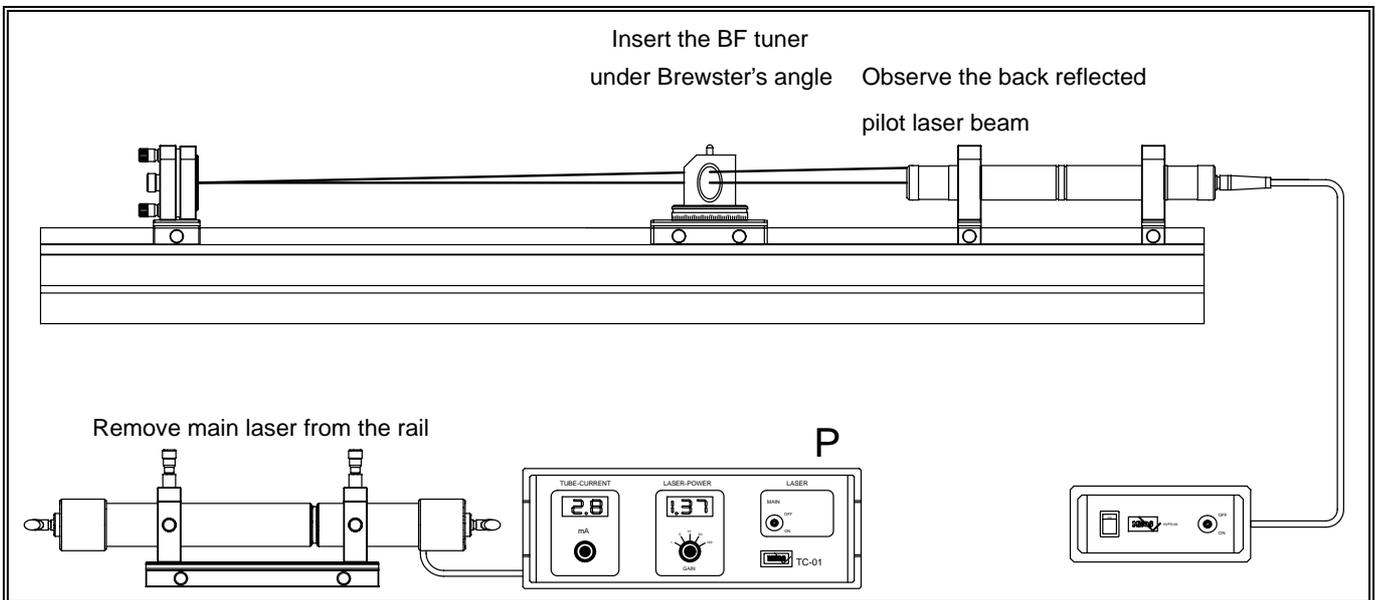these beams to the exit of the pilot laser and you will also observe interference fringes. Note that nearly all laser mirror do have a so called wedge. This means that the plan backside has a small angle deviation with respect to the front side. The wedge shall prevent an unwanted etalon effect. Although the laser mirror aligned by the above described method the front side is not unambiguously aligned properly with respect to the laser axis. This problem can be solved, when the right laser mirror holder is turned by 180° in such a way that the coated side of the laser mirror faces the pilot laser. Once aligned the holder is turned back to the required position.
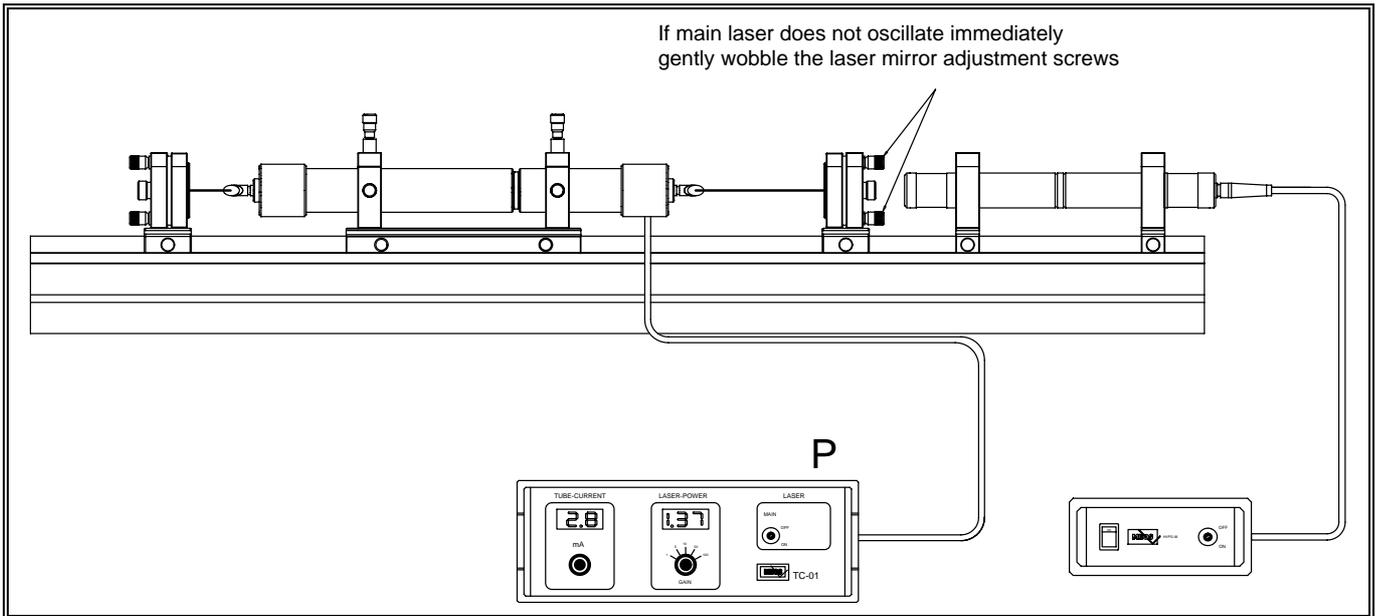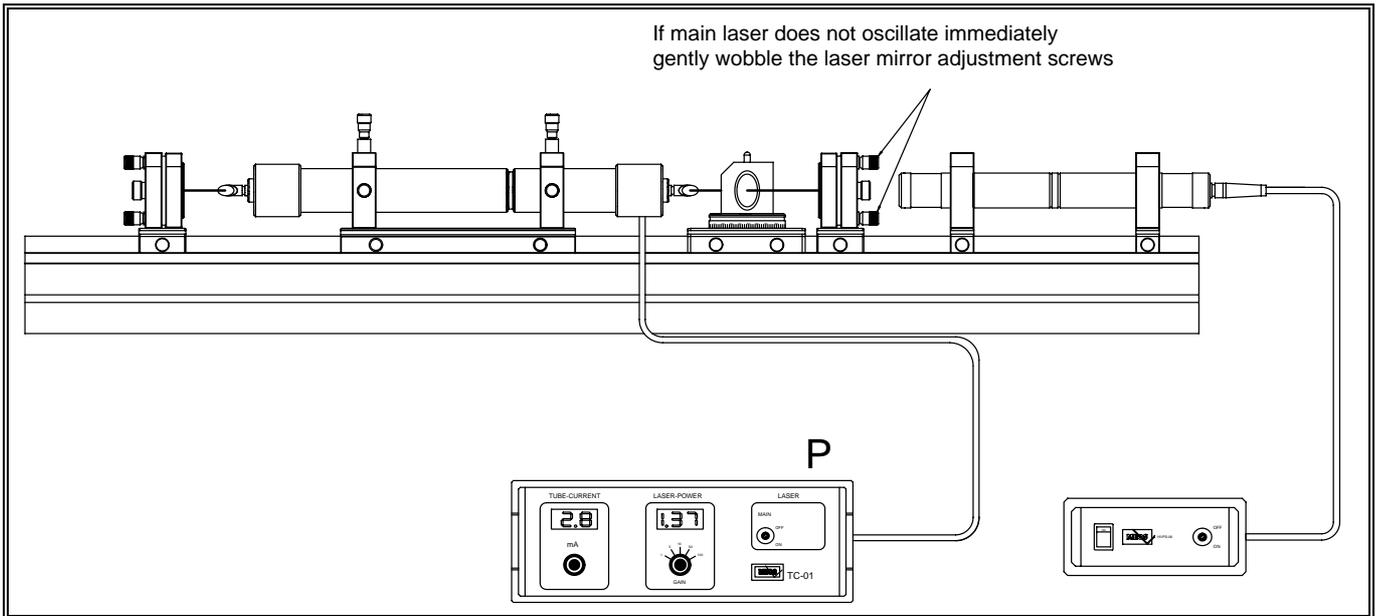
When all the previous steps are done properly you can now start the main laser to oscillation. Proceed as following: Switch the pilot laser off and the main laser on. If the first steps were done properly the laser will start more or less strong oscillating immediately. When not, note the position in mind of the upper adjustment screw and wobble it a little bit. you should observe now flashing up of the laser. If this fails, return to the initial position of the screw. Try the same with the lower one. When no other reasons

for failure are existing the laser should now show flashing when wobbling the screw. In this case turn the screw to stable oscillation. Realign the upper screw for highest laser power. Realign the left mirror holder for best output. If still no lasing action will occur, do not waist your time and start the alignment process from the beginning. Because now all components are prealigned, this will be done in a few minutes. Make sure that all optics are cleaned and you are using the right mirrors !

## 5.2 Alignment of the birefringent Tuner

If main laser does not oscillate immediately gently wobble the laser mirror adjustment screws
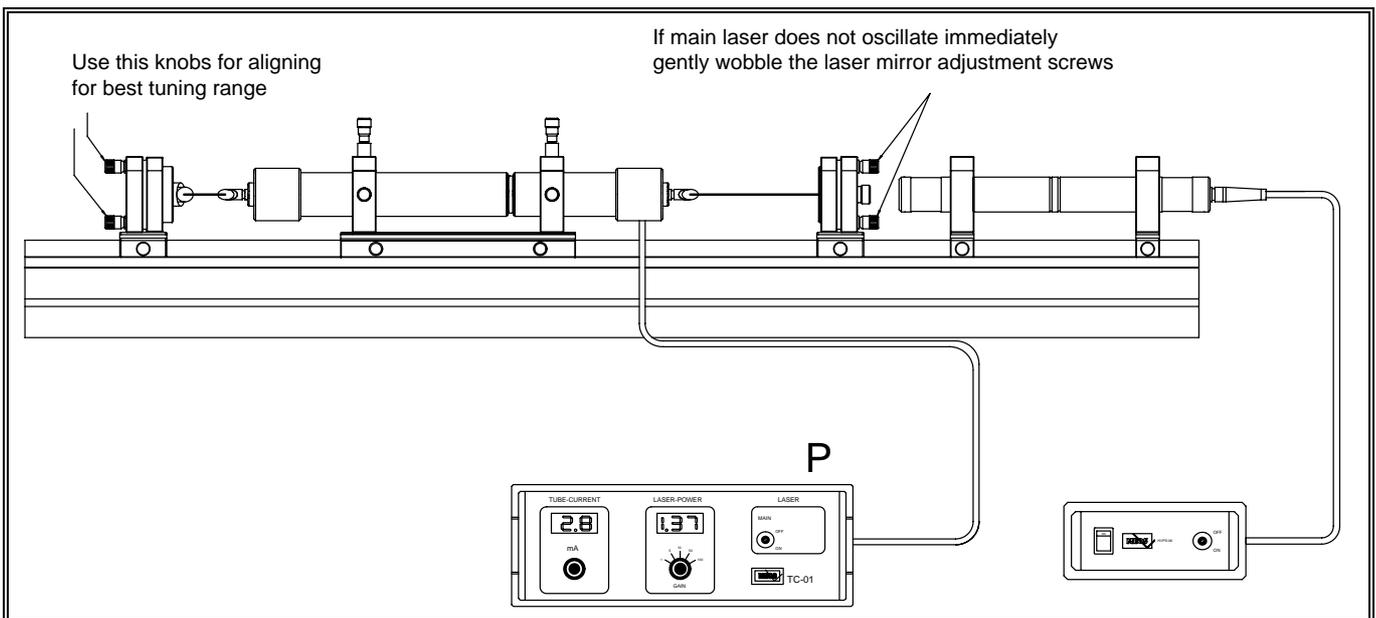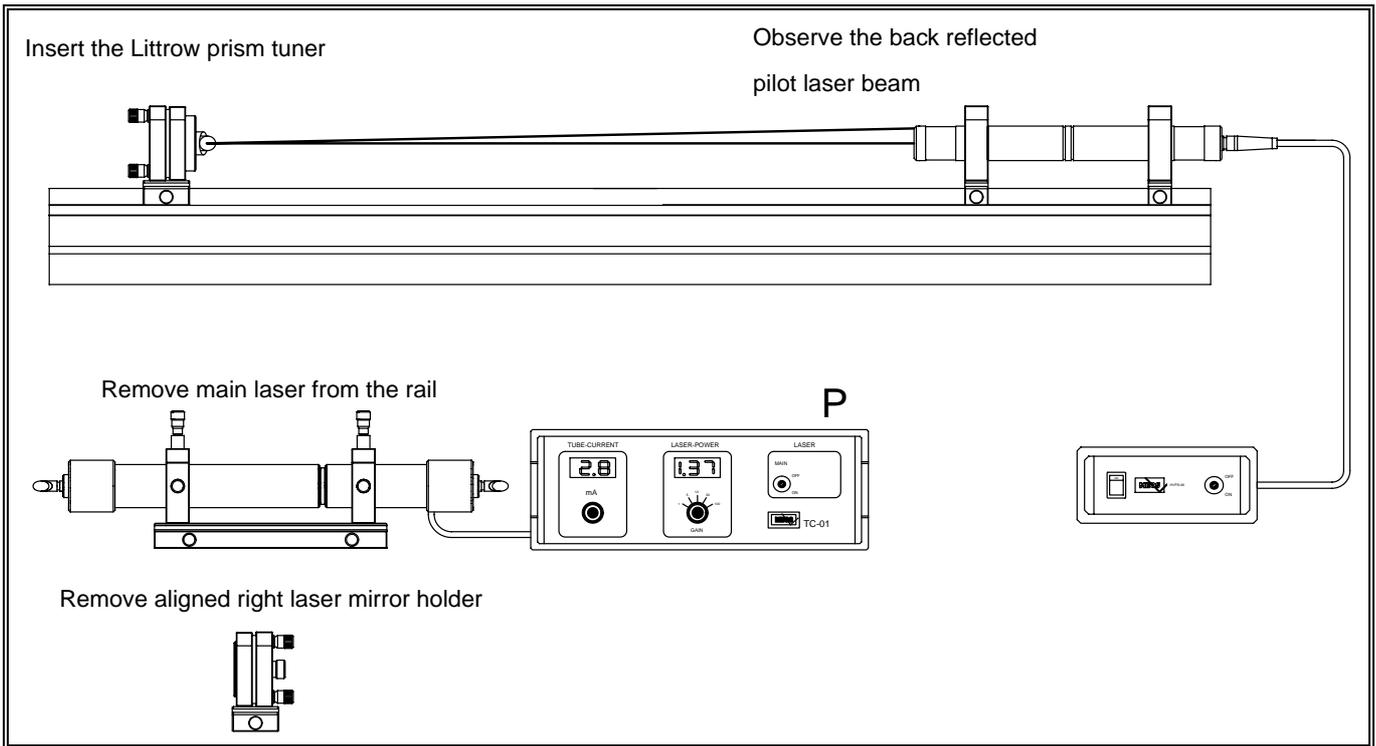
The tuning element consists of a natural quartz plate app. 1 mm thick. When the BFT is placed into the resonator it causes a beam displacement. Therefore it is necessary to repeat the primary alignment when the tuner is used. It is also possible to insert the tuner into the resonator without carrying out the primary alignment. Proceed as following: Align the laser to highest power. Turn the birefringent tuner so that the plate will be perpendicular to the laser axis. Rotate the plate around its optical axis into a position where laser oscillation occurs again. Realign the laser again. Now turn the plate in direction to the Brewster´s angle. Do it in some steps. After each step realign the laser. In the vicinity of the Brewster´s angle the laser shows considerable increase of intensity. You also can find this position when the intensity of the reflected beam from the BFT plate shows a minimum. If now the plate is rotated around its optical axis the main line (632.8 nm) will occur 3 to four times. Select the best one and realign the laser for best operation. When you tune in the vicinity of the main line at 632 nm you will find 5 different lines at the following wavelength and relative strength:

| 1. | 611.8 nm | 10 |
|----|----------|-----|
| 2. | 629.8 nm | 20 |
| 3. | 632.8 nm | 100 |
| 4. | 635.2 nm | 6 |
| 5. | 640.1 nm | 34 |

The orange line at 611.8 nm as well the line at 635.2 nm are sensitive to additional losses due to pollution on the optics. Clean them again when you will not find these lines. Especially the windows of the tube and the BFT plate are exposed to pollution because the electrical field of the laser beam on their surfaces is not zero as on the mirrors. Once the orange line is oscillating realign the laser resonator and optimise the Brewster angle by turning slightly the BFT. Note that the line can vanish and will return by tuning slightly the plate

## 5.3 Alignment of the Littrow Prism Tuner

Insert the Littrow prism tuner

Observe the back reflected

pilot laser beam

Remove main laser from the rail

P

TUBE-CURRENT     LASER-POWER     LASER

2.8
mA

1.37
GAIN

MAIN
OFF
ON

TC-01

OFF
ON

Remove aligned right laser mirror holder

Use this knobs for aligning
for best tuning range

If main laser does not oscillate immediately
gently wobble the laser mirror adjustment screws

P

TUBE-CURRENT     LASER-POWER     LASER

2.8
mA

1.37
GAIN

MAIN
OFF
ON

TC-01

OFF
ON

The LPT is a combined optical component consisting of a coated prism. It acts as laser mirror and selective element simultaneously. Remove the left and right laser mirror holder and the main laser module from the rail after aligning for best operation. Insert the Littrow prism module onto the rail as shown above. The Littrow prism is pre-aligned in its holder. Adjust the LPT by means of the pilot laser as done earlier in the section primary alignment. Put the right laser mirror adjustment holder onto the optical rail. This mirror should be prealigned from the previous alignment. Switch the pilot laser off and the main laser on. If the main laser does not oscillate immediately wobble the laser mirror adjustment screws as shown before. In this set-up the proper alignment of the LPT is more important than that of simple mirrors. Carry out the alignment steps more carefully you are used to do before. Once the laser is started you realign for best operation. The lower adjustment screw tilts the prism for the desired tuning. May be you are surprised, that at the first try no tuning occurs. When you look to the spot of the laser beam on the right mirror you will observe that the spot is moving when the prism is tilted. The main line does not want do decease to let other lines run. At this point you will realise the advantage of a BFT for separating narrow lines especially with relative short resonators. However to achieve oscillation on the orange line one has to carry out a so called beam wandering technique. This means the path of the laser beam inside the resonator can be changed by turning adja-

cent adjustment screws. The path for the dominant red line is changed in such a way, that the losses will increase, but favour the orange "path". This is been done by searching.

Each system has been checked to run on the orange line tuned by the LPT.

## 5.4 Alignment of the Fabry-Perot Etalon



If main laser does not oscillate immediately gently wobble the etalon adjustment screws

P
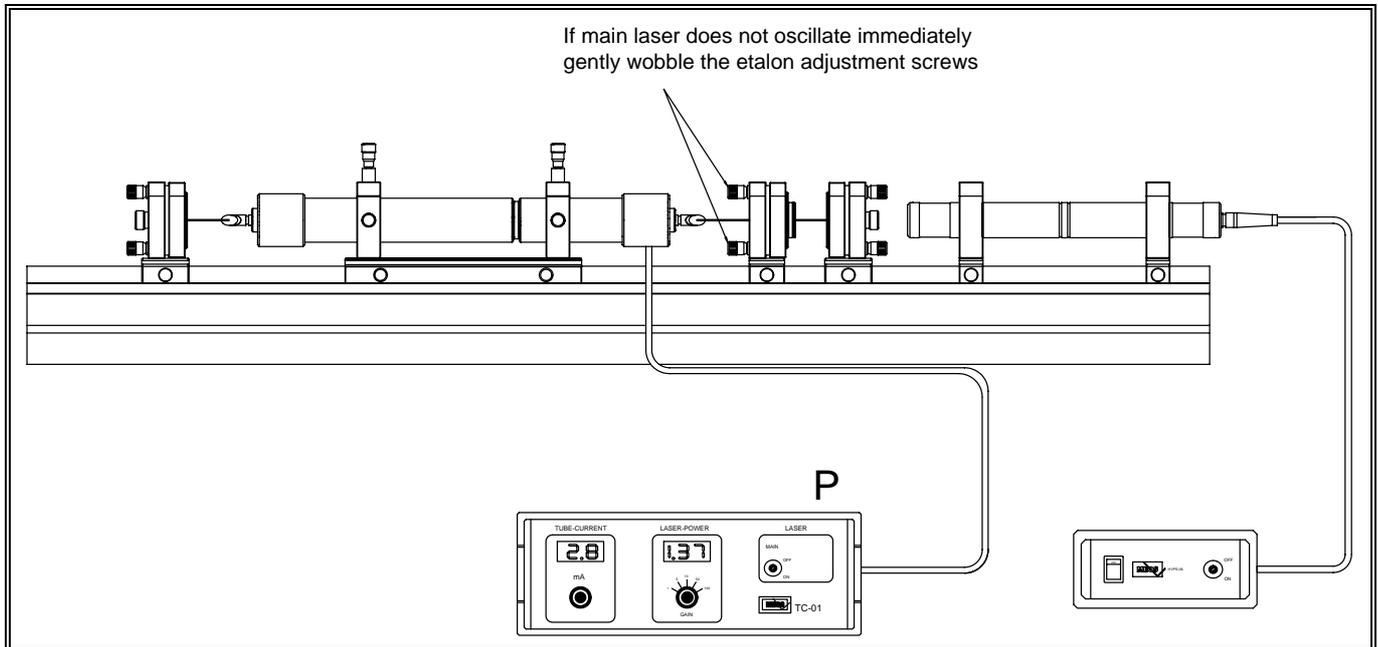
Place the etalon module onto the rail as shown above. The etalon itself consists of a high precision quartz plate with a thickness of 10 mm. The parallel faces are not coated. The Fresnel losses of app. 4% per face are sufficient for the needed Finesse. Before inserting the etalon module make sure that the adjustable part it is aligned parallel to the fixed one. Inspection by sight is sufficient.

In this case the etalon also is aligned perpendicular to the laser axis. Instant more or less strong laser oscillation should occur when the etalon is inserted.

Observe the back reflections of the etalon on the front face of the right laser mirror holder. If the etalon is not aligned perfectly perpendicular (zero order) one will notice several spots.

Align it to the zero order, that means all back reflections must be centred into the main laser beam. With one of the adjustment screws, favourable the upper one, the etalon may now be tilted.

One observes different positions for which laser oscillation again occurs. The check if the laser is running in single mode can be done with an external Fabry Perot, for instance the with the set-up of EXP03 (Fabry-Perot).
If one uses the laser mirror holder of the mentioned experiment with the piezo electric transducer (PZT) the single mode can also be checked.
In addition the observation of the lamb dip is possible.

## 5.5  The tube controller TC 01

The tube controller supplies the main laser and the pilot laser with the needed high voltage. For the main laser the current of the high voltage supply can be varied in a range from 5 to 8 mA in order to optimise the laser power for the different lines.
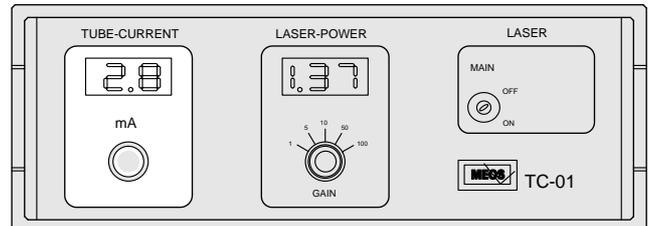
# Controller TC-01

The controller unit TC-01 serves two purposes. It provides the high voltage for the main HeNe-Laser tube and contains a the photodiode amplifier for the measurement of the relative output power of the laser.
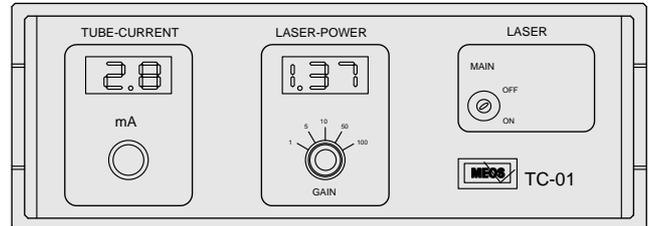
# Discharge current

The nominal current of the laser tube is 5 mA. Only for special measurements the laser tube should be used at higher values of the current. By means of the control button, the discharge current can be adjusted between 4.8 and 7.5 mA. The current is read in mA.

# Laser power

The input of the photodiode amplifier is at the rear of the controller unit. The photodetector (Module F) is connected by means of the BNC-cable which comes along with the detector. The reading can not be done in absolute power units. In so far it is only an adjustment aid for weak spectral lines respectively a tool for relative power measurements.
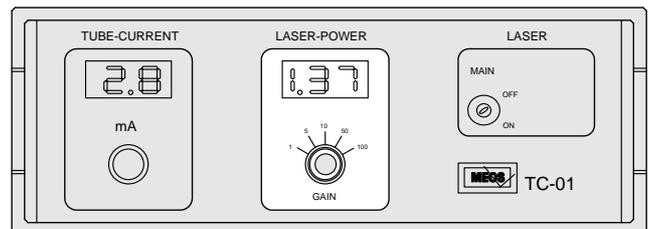
# Key switch

The key switch at the front panel prevents unauthorised switching on of the laser.
The main switch, the mains connection and the mains fuse are an integral unit at the rear of the controller.